Two-Gluon Exchange Graphs in Cavity QCD to Order α_S^2

Marc Schumann
Institute of Theoretical Physics and Astrophysics
University of Cape Town

A thesis submitted in fulfillment
of the requirements for the degree of
Master of Science in Theoretical Physics

January 1998

Contents

Chapter 1

Introduction

Quantum chromodynamics (QCD) was introduced in 1973 by Fritzsch, Gell-Mann and Leutwyler [1] to describe the dynamics of strongly interacting particles. In the late sixties, through work by Friedmann, Kendall [2], Taylor [3] and others on deep inelastic scattering of electrons off nucleon targets, it had become evident that all hadrons consist of point-like 'partons', which have been identified as quarks and gluons. Due to the discovery of Bjorken scaling, proposed in 1969 [4] and experimentally verified soon afterwards, a theory was needed that would allow the partons to behave like free particles when investigated at large momentum transfers, corresponding to small distances. Gross and Wilczek [5, 6] and Politzer [7] showed in 1973 that asymptotic freedom is indeed a property of non-Abelian gauge field theories. Conveniently, it had just been shown by 't Hooft that non-Abelian, or Yang-Mills field theories are renormalizable [8, 9]. QCD is such a renormalizable and asymptotically free field theory, in which the non-Abelian gauge fields describe the gluons, the carrier of the strong interaction.

Asymptotic freedom allows for perturbative calculations at high energies. Precise tests of QCD could be done at low energies, however, due to the running coupling constant, perturbative calculations of low-energy QCD are rather unreliable, if not altogether impossible. Another problem arises due to the interaction between gluons. With increasing order of the perturbation expansion, the number of Feynman graphs grows much faster than in quantum electrodynamics (QED), where the gauge fields, the photons, are not self-interacting. High precision tests have been done for QED,

for example, measurements of the anomalous magnetic moment of the electron agree with the theory to 9 digits.

A further requirement of a theory describing the strong interactions is that it must produce confinement of the colour carrying particles, the quarks and gluons. So far, it has not been possible to prove that QCD actually yields confinement, even though the coupling constant grows rapidly for distances approaching 1 fm and larger, which is of the order of the size of a hadron. It appears that confinement is a non-perturbative consequence of QCD. Ongoing and future experiments involving collisions of heavy nuclei are designed for the search of deconfinement and the creation of a quark-gluon plasma. Conclusive results on the experimental side of deconfinement are not expected before the "large" particle accelerator like the Relativistic Heavy Ion Collider (RHIC) at Brookhaven go online in late 1999.

One can resort to artificially introducing confinement into the free theory using a phenomenological model. This can be done in many ways [10, 11, 12, 13, 14, 15, 16], but the simplest way to achieve confinement of quarks and gluons is the MIT bag model [17, 18, 19, 20], in which boundary conditions are imposed on the colour carrying fields at an arbitrary (but for convenience usually spherical) spacelike surface. This model has been quite popular, as it allows the calculation of, for example, the masses of baryons and mesons with only a few free parameters and with little deviation from the experimentally measured values. This is relatively surprising, since confining the particles to a static sphere breaks the translational and the Lorentz invariance, as well as the chiral symmetry of the theory. Furthermore, there remains a possibility that confinement is already contained in the original theory of QCD. Nevertheless, this model has the major advantage that by imposing boundary conditions on the field operators, only a minimal number of modifications yields confinement, while at the same time one retains most of the properties of the underlying gauge theory.

Confined QCD has been approached from a different angle by Buser *et al.* [21] by showing that one can formulate QCD consistently in a finite volume subject to the MIT bag model boundary conditions. Stoddart *et al.* [22, 23, 24, 25] have introduced renormalization techniques to this theory. One can therefore see cavity QCD as a fully fledged field theory in its own right. Calculations of the quark self-energy for

massless [23] and massive quarks [26, 27], the gluon self-energy [28, 29, 30], the magnetic moments of nucleons and many other hadrons [31, 32, 33] and the ratio of g_A/g_V [34, 35] have been performed in the framework of cavity QCD.

The purpose of this thesis is to go beyond the usual first order calculations and to evaluate the two-gluon exchange diagrams, which are second order in α_S. Two distinct Feynman diagrams exist, of which each consists of twenty-four time-ordered diagrams. All the possible time-ordered diagrams are calculated here. A similar calculation of only the first six time-ordered diagrams has been performed by Stoddart *et al.* [36, 37].

This thesis is structured as follows: In the second chapter the classical locally gauge invariant theory is quantized using the canonical operator formalism, following closely the steps taken by Buser *et al.* [21]. The boundary conditions of the MIT bag model are then introduced and the quark and gluon propagators are presented. The chapter closes with a brief overview of the Gell-Mann and Low theorem and the perturbative expansion of the energy shift in symmetrical form. In the third chapter, the calculations of the energy shift due to first- and second-order gluon-exchange diagrams are performed in detail. The first order is included since it is a helpful introductory example for the more tedious calculations for the higher-order diagrams. The results are compared to those obtained by Stoddart *et al.* [36, 37]. In chapter four, the results are inserted into the mass formula of the MIT bag model and the mass spectrum of strange and non-strange hadrons is calculated and compared to the experimental values. Finally, in chapter five, a conclusion is drawn from the results and a brief outlook into possible extensions of the work done here is given. The appendices follow, containing the derivation of the cavity modes of quarks and gluons in Appendix A, the quark-gluon vertex integrals in Appendix B, a brief introduction into the numerical methods in Appendix C, and the energy denominators for all the time-ordered diagrams in Appendix D.

Chapter 2

Free Space and Cavity QCD

To introduce cavity QCD, it is necessary to give a brief review of some of the more familiar properties of QCD in free space. This exercise also serves the purpose of setting the notation used in the calculations in the later chapters.

Cavity QCD follows quite easily from the free-space theory since the only major change is the introduction of a set of boundary conditions. These boundary conditions do not affect the basic algebra of the fields, but simply change the functional form and some internal properties of the wave functions. A very nice account of the derivation of the wave functions is given in the book by Greiner and Schäfer [38, Chapter 3.3]. The notation used in this section follows, however, more closely that of Buser *et al.* [21] and Lindebaum [33].

2.1 Canonical Quantization

The Lagrange density of QCD is given by

$$\mathcal{L} = \bar{\psi}\left(i\gamma_\mu D^\mu - M\right)\psi - \frac{1}{2}i\partial_\mu\left(\bar{\psi}\gamma^\mu\psi\right) - \frac{1}{4}\boldsymbol{F}_{\mu\nu}\boldsymbol{F}^{\mu\nu} - \frac{1}{2}\lambda\partial_\mu\boldsymbol{A}^\mu\cdot\partial_\nu\boldsymbol{A}^\nu + i\boldsymbol{\chi}\cdot\partial_\mu\mathcal{D}^\mu\boldsymbol{\omega}. \tag{2.1}$$

The interactions between the quark field ψ, the gluon fields $\boldsymbol{A}^\mu$, and the ghost fields $\boldsymbol{\omega}$, are contained in the covariant derivatives

$$D^\mu\psi = \left(\partial^\mu - ig\frac{\boldsymbol{\lambda}}{2}\cdot\boldsymbol{A}^\mu\right)\psi, \tag{2.2}$$

$$\mathcal{D}^\mu\boldsymbol{\omega} = \partial^\mu\boldsymbol{\omega} + g\boldsymbol{A}^\mu\times\boldsymbol{\omega} \tag{2.3}$$

respectively. The chromoelectromagnetic field strength tensor $\boldsymbol{F}^{\mu\nu}$ is defined as

$$\boldsymbol{F}^{\mu\nu} = \partial^\mu \boldsymbol{A}^\nu - \partial^\nu \boldsymbol{A}^\mu + g\boldsymbol{A}^\mu \times \boldsymbol{A}^\nu \tag{2.4}$$

and is related, analogously to QED, to the covariant derivative, Equation (2.2), via the Bianchi identity

$$[D^\mu, D^\nu] = -\frac{1}{2} ig\boldsymbol{\lambda} \cdot \boldsymbol{F}^{\mu\nu}. \tag{2.5}$$

The scalar and vector products are defined in the eight dimensional colour space as

$$\boldsymbol{A} \cdot \boldsymbol{B} = \sum_{a=1}^{8} A_a B_a, \tag{2.6}$$

$$(\boldsymbol{A} \times \boldsymbol{B})_a = \sum_{b,c=1}^{8} f_{abc} A_b B_c, \tag{2.7}$$

where the f_{abc} are the structure constants of $\mathrm{SU}(3)_{\mathrm{colour}}$ and the λ_a, $(a = 1, \ldots, 8)$ are the Gell-Mann matrices. The first term of the Lagrange density (2.1) describes the locally gauge-invariant interaction of quarks and gluons. The second and third terms are kinetic terms for the quarks and gluons. The fourth term, which contains the gauge parameter λ, is a globally gauge-invariant covariant gauge fixing term, which is required to make the canonical momentum $\boldsymbol{\Pi}^0$ of $\boldsymbol{A}^0$ non-vanishing. The last term is the Faddeev-Popov ghost term [39] which makes the Lagrange density invariant under Becchi-Rouet-Stora (BRS) transformation [40].

Since it is not known how to apply the usual method of Feynman path integrals [41] to the cavity, the canonical operator formalism is used. The Hamilton density therefore has to be derived from the Lagrangean, which is done by replacing the derivatives of the fields in the Lagrangean by the canonical conjugate momenta and using

$$\mathcal{H} = -\frac{\partial \mathcal{L}}{\partial \dot{\psi}} \dot{\psi} + \dot{\bar{\psi}} \frac{\partial \mathcal{L}}{\partial \dot{\bar{\psi}}} + \dot{\boldsymbol{A}}_\mu \cdot \frac{\partial \mathcal{L}}{\partial \dot{\boldsymbol{A}}_\mu} + \dot{\boldsymbol{\chi}} \cdot \frac{\partial \mathcal{L}}{\partial \dot{\boldsymbol{\chi}}} + \dot{\boldsymbol{\omega}} \cdot \frac{\partial \mathcal{L}}{\partial \dot{\boldsymbol{\omega}}} - \mathcal{L}. \tag{2.8}$$

The minus sign on the first term is due to the Grassmann nature of the quark field. The conjugate momenta of the fields are:

$$\Psi = \frac{\partial \mathcal{L}}{\partial \dot{\psi}} = -\frac{1}{2} i\psi^\dagger \tag{2.9}$$

$$\bar{\Psi} = \frac{\partial \mathcal{L}}{\partial \dot{\bar{\psi}}} = -\frac{1}{2} i\bar{\psi}^\dagger \tag{2.10}$$

$$\boldsymbol{\Pi}^k = \frac{\partial \mathcal{L}}{\partial \dot{\boldsymbol{A}}_k} = \boldsymbol{F}^{k0} \qquad k = 1, 2, 3 \tag{2.11}$$

$$\boldsymbol{\Pi}^0 = \frac{\partial \mathcal{L}}{\partial \dot{\boldsymbol{A}}_0} = -\lambda \partial_\mu \boldsymbol{A}^\mu \tag{2.12}$$

$$\boldsymbol{X} = \frac{\partial \mathcal{L}}{\partial \dot{\boldsymbol{\chi}}} = -i\mathcal{D}_0 \boldsymbol{\omega} \tag{2.13}$$

$$\boldsymbol{\Omega} = \frac{\partial \mathcal{L}}{\partial \dot{\boldsymbol{\omega}}} = i\dot{\boldsymbol{\chi}}. \tag{2.14}$$

Equation (2.12) shows clearly that the zeroth component of the canonical conjugate momentum of the gluon field would vanish if the gauge fixing term was not present in the Lagrange density.

The Hamiltonian density can be written as the sum of two terms

$$\mathcal{H} = \mathcal{H}_0 + \mathcal{H}_{\text{int}}. \tag{2.15}$$

The first term $\mathcal{H}_0$ contains the free fields and is independent of the strong coupling constant g, and is given by

$$\begin{aligned} \mathcal{H}_0 = {} & \bar{\psi}\left(-\frac{1}{2} i\gamma_k \overleftrightarrow{\partial^k} + M\right)\psi + \frac{1}{4}\left(\partial_k \boldsymbol{A}^l - \partial_l \boldsymbol{A}^k\right)\cdot\left(\partial_k \boldsymbol{A}^l - \partial_l \boldsymbol{A}^k\right) + \frac{1}{2}\boldsymbol{\Pi}^k \cdot \boldsymbol{\Pi}^k \\ & -\frac{1}{2\lambda}\boldsymbol{\Pi}^0 \cdot \boldsymbol{\Pi}^0 + \boldsymbol{\Pi}^k \cdot \partial_k \boldsymbol{A}^0 - \boldsymbol{\Pi}^0 \cdot \partial_k \boldsymbol{A}^k - i\boldsymbol{\Omega}\cdot\boldsymbol{X} - \partial_k \boldsymbol{\chi}\cdot\partial_k \boldsymbol{\omega}. \end{aligned} \tag{2.16}$$

The second term $\mathcal{H}_{\text{int}}$ is the interaction Hamiltonian density and explicitly depends on g, and is given by

$$\begin{aligned} \mathcal{H}_{\text{int}} = {} & -\frac{1}{2} g\bar{\psi}\gamma_\mu \boldsymbol{\lambda}\psi \cdot \boldsymbol{A}^\mu - \frac{1}{2} g\left(\partial_k \boldsymbol{A}^l - \partial_l \boldsymbol{A}^k\right)\cdot\left(\boldsymbol{A}^k \times \boldsymbol{A}^l\right) \\ & -g\boldsymbol{\Pi}^k \cdot \left(\boldsymbol{A}^k \times \boldsymbol{A}^0\right) + \frac{1}{4} g^2 \left(\boldsymbol{A}_k \times \boldsymbol{A}_l\right)\cdot\left(\boldsymbol{A}^k \times \boldsymbol{A}^l\right) \\ & +g\boldsymbol{\Omega}\cdot\left(\boldsymbol{A}^0 \times \boldsymbol{\omega}\right) + ig\partial_k \boldsymbol{\chi}\cdot\left(\boldsymbol{A}^k \times \boldsymbol{\omega}\right). \end{aligned} \tag{2.17}$$

The different terms in the interaction Hamiltonian density $\mathcal{H}_{\text{int}}$ describe the interaction between two quarks and a gluon, between three gluons, between four gluons, and between two ghosts and a gluon. The Hamiltonian is then found by integrating the Hamiltonian density over the spatial coordinates,

$$H(t) = H_0(t) + H_{\text{int}}(t) = \int d^3x \Big(\mathcal{H}_0(\vec{x}, t) + \mathcal{H}_{\text{int}}(\vec{x}, t)\Big). \tag{2.18}$$

The Hamiltonian can now be quantized by interpreting the classical fields as field operators and imposing equal-time anticommutation relations on the fields that are Grassmann in the classical theory, and commutation relations on the Hermitian

gluon (i.e. gauge boson) field operators.

$$\begin{aligned}
\left\{\psi_{c,f,\alpha}(\vec{x},t),\psi^{\dagger}_{c',f',\alpha'}(\vec{y},t)\right\} &= \delta_{cc'}\delta_{ff'}\delta_{\alpha\alpha'}\delta^3(\vec{x}-\vec{y}) \\
\{\omega_a(\vec{x},t),\boldsymbol{\Omega}_b(\vec{y},t)\} &= -i\delta_{ab}\delta^3(\vec{x}-\vec{y}) \\
\{\chi_a(\vec{x},t),\boldsymbol{X}_b(\vec{y},t)\} &= -i\delta_{ab}\delta^3(\vec{x}-\vec{y}) \\
[\boldsymbol{A}^{\mu}_a(\vec{x},t),\boldsymbol{\Pi}^{\nu}_b(\vec{y},t)] &= ig^{\mu\nu}\delta_{ab}\delta^3(\vec{x}-\vec{y}).
\end{aligned} \tag{2.19}$$

All commutators of the gluon field operators, all anticommutators of the quark and ghost field operators and all commutators involving two different types of field operators not written down explicitly, are understood to vanish.

The fields have now become field operators in the Heisenberg picture. They satisfy the Heisenberg equation of motion

$$i\frac{\partial}{\partial t}F(\vec{x},t) = [F(\vec{x},t),H], \tag{2.20}$$

while the state vectors defining the Fock space are time independent. In the context of cavity QCD, it is useful to transform the operators and states to the interaction or Dirac picture. This can be done by applying a unitary transformation $U(t)$ to vectors and operators in the Fock space which satisfies the differential equation

$$i\frac{\partial}{\partial t}U(t) = U(t)H_{\rm int} \tag{2.21}$$

together with the initial condition $U(0) = 1$. The Heisenberg states $|\psi\rangle$ are then transformed into Dirac states $|\hat{\psi}(t)\rangle$ by

$$|\hat{\psi}(t)\rangle = U(t)|\psi\rangle. \tag{2.22}$$

A Heisenberg operator $F(\vec{x},t)$, which depends on $\vec{x}$ and t via the field operators, their spatial derivatives. and their canonical conjugate momenta, is transformed from the Heisenberg to the Dirac picture according to

$$\hat{F}(\vec{x},t) = U(t)F(\vec{x},t)\,U^{-1}(t). \tag{2.23}$$

The anti-commutation and commutation relations (2.19) still hold in the Dirac picture. The equations of motion for the operators and for the state vectors are

$$i\frac{\partial}{\partial t}\hat{F}(\vec{x},t) = \left[\hat{F}(\vec{x},t),\hat{H}_0\right], \tag{2.24}$$

$$i\frac{\partial}{\partial t}|\hat{\psi}(t)\rangle = \hat{H}_{\rm int}|\hat{\psi}(t)\rangle, \tag{2.25}$$

respectively. According to Equation (2.24), the field operators satisfy the non-interacting field equations

$$(i\gamma_\mu \partial^\mu - m)\,\hat{\psi} = \hat{\bar{\psi}}(i\gamma_\mu \overleftarrow{\partial^\mu} + m) = 0, \tag{2.26}$$

$$\Box \hat{A}^\mu + (\lambda - 1)\partial^\mu \partial_\nu \hat{A}^\nu = 0, \tag{2.27}$$

$$\Box \hat{\omega} = \Box \hat{\chi} = 0. \tag{2.28}$$

There remains one problem, namely that covariant canonical quantization of gauge fields leads to a Fock space with indefinite metric, i.e. there are states with negative norm. This can be seen, if one looks at the commutator

$$[A^\mu, \Pi^\nu] = i g^{\mu\nu} \tag{2.29}$$

which results in

$$[c^\mu, c^{\nu\dagger}] = -g^{\mu\nu} \tag{2.30}$$

for the creation and annihilation operators. Therefore, one has, for example, a state

$$|1\rangle = c^{0\dagger}|0\rangle, \qquad \text{but } \langle 1|1\rangle = -\langle 0|0\rangle. \tag{2.31}$$

The problem clearly arises from the dependence of the norm on the Minkowski metric of space-time $g^{\mu\nu}$, and it results in negative probabilities. One needs to introduce a further condition to restrict the Fock space to the physical world. The procedure is similar to QED, where one has the Gupta-Bleuler condition [42, 43]

$$\partial_\mu A^{\mu(+)}|\psi_{\text{phys}}\rangle = 0 \tag{2.32}$$

to guarantee that the subspace $\{|\psi_{\text{phys}}\rangle\}$ has a positive definite norm. The corresponding relation in QCD is that the BRS charge of the physical states vanishes [44],

$$Q_{\text{BRS}}|\psi_{\text{phys}}\rangle = 0. \tag{2.33}$$

The BRS charge is the spatial integral of the zeroth component of the conserved current which is due to the BRS invariance of the Lagrange density.

The properties of QCD discussed so far, apply regardless of the volume occupied by the fields. It is now fitting to consider only a finite volume of space and move on to cavity QCD.

2.2 Cavity Quantum Chromodynamics

The confinement of colour-carrying particles is imposed on the free-space theory by introducing boundary conditions on an arbitrary, but for convenience spherical, space-like surface S. The boundary conditions chosen are those of the MIT bag model [17, 18, 19] which are linear in the field operators and independent of the strong coupling constant. They confine the colour-carrying fields into a spherical 'bag' or cavity and preserve the BRS symmetry of the theory [21]. The boundary conditions are

$$\left(in_k\gamma^k - 1\right)\hat{\psi}\Big|_S = i\hat{\bar{\psi}}\left(in_k\gamma^k + 1\right)\Big|_S = 0, \tag{2.34}$$

$$n_k\left(\partial^k\hat{A}^\nu - \partial\nu\hat{A}_k\right)\Big|_S = n_k\hat{A}^k\Big|_S = n_k\partial^k\left(\partial_\nu\hat{A}^\nu\right)\Big|_S = 0, \tag{2.35}$$

$$n_k\partial^k\hat{\omega}\Big|_S = n_k\partial^k\hat{\chi}\Big|_S = 0. \tag{2.36}$$

The vector $n^\mu = (n^0, \vec{x})$ denotes a spacelike unit vector

$$n^\mu n_\mu = -1, \tag{2.37}$$

where $\vec{n}$ is perpendicular to the cavity surface $\mathcal{S}$ and pointing outward. The solutions of the non-interacting field equations (2.26)–(2.28), subject to the above boundary conditions, are the cavity modes discussed in Appendix A. One should note, that the spherical symmetry of the bag surface is only the most convenient choice. One can also choose, for instance, a spheroidal surface, as has been done by Viollier *et al.* [45].

2.2.1 The Quark Propagator

The quark field operator can be expanded in the complete set of quark cavity modes. The operator character of the field operators is then carried by the expansion coefficients. The quark field operator is

$$\hat{\psi}_{cf}(x) = \sum_{\substack{\kappa,\mu \\ \nu>0}}\left(\hat{a}_{cfn}u_n(\vec{x})e^{-i\varepsilon_n t} + \hat{b}^\dagger_{cfn}u_{-n}(\vec{x})e^{i\varepsilon_n t}\right), \tag{2.38}$$

where n denotes the set of quantum numbers $n = \{\nu, \kappa, \mu\}$, which are the radial, Dirac and magnetic quantum numbers, respectively. There is an implicit dependence of the cavity modes on the flavour of the quark due to the flavour dependence of the

quark masses. The set of quantum numbers $-n$ is defined as $-n = \{-\nu, -\kappa, -\mu\}$. The operators $\hat{a}^{\dagger}_{cfn}$ and $\hat{a}_{cfn}$ are the quark creation and annihilation operators which create and annihilate a quark with the quantum numbers c, f, n. The operators $\hat{b}^{\dagger}_{cfn}$ and $\hat{b}_{cfn}$ are the antiquark creation and annihilation operators. The spinors $u_n(\vec{x})$ are the quark cavity modes as given in Appendix A. The quark field operator satisfies the anti-commutation relation (2.19) and it reduces to the anti-commutation relation of the quark/antiquark creation and annihilation operators

$$\left\{\hat{a}_{cfn}, \hat{a}^{\dagger}_{c'f'n'}\right\} = \left\{\hat{b}_{cfn}, \hat{b}^{\dagger}_{c'f'n'}\right\} = \delta_{cc'}\delta_{ff'}\delta_{nn'}. \tag{2.39}$$

The cavity quark propagator is defined as the time-ordered product of the fields

$$iS\left(x, x'\right) = \left\langle \hat{0} \left| T\left[\hat{\psi}_{cf}(x)\hat{\bar{\psi}}_{c'f'}(x')\right] \right| \hat{0} \right\rangle. \tag{2.40}$$

Substituting the quark field operator (2.38) into this expression and using the anti-commutation relations (2.39), one obtains

$$iS\left(x, x'\right) = \delta_{cc'}\delta_{ff'} \sum_{\substack{\kappa,\,\mu \\ \nu\,>\,0}} \left[u_n(\vec{x})\bar{u}_n(\vec{x}')\theta(t-t') - u_{-n}(\vec{x})\bar{u}_{-n}(\vec{x}')\theta(t'-t)\right] e^{-i\varepsilon_n|t-t'|}. \tag{2.41}$$

This expression can be written more compactly as

$$iS\left(x, x'\right) = i\delta_{cc'}\delta_{ff'} \sum_{\kappa\nu\mu} u_n(\vec{x})\bar{u}_n(\vec{x}') \int \frac{d\omega}{2\pi} \frac{e^{-i\omega(t-t')}}{\omega - \varepsilon_n \pm i0} \tag{2.42}$$

by using the integral representation of the theta function

$$\theta(t) = \lim_{\varepsilon \to 0} \frac{-1}{2\pi i} \int_{-\infty}^{\infty} d\omega \frac{e^{-i\omega t}}{\omega + i\varepsilon}. \tag{2.43}$$

The sum now ranges over both positive and negative radial quantum numbers ν. The usual Feynman prescription for the poles is used. Poles with positive (negative) energy ε_n acquire a small negative (positive) imaginary part. The propagator is, of course, a Green's function of the Dirac equation

$$(i\partial\!\!\!/_x - m)S(x, y) = \delta^{(4)}(x, y). \tag{2.44}$$

2.2.2 The Gluon Propagator

The gluon field operator can be expanded similarly to the quark field operator in terms of the gluon cavity modes as

$$\hat{A}_a^\mu(x) = \sum_{m\Sigma} \frac{1}{\sqrt{2\Omega_m^\Sigma}} \left[\hat{c}_{am}^\Sigma a_{m\Sigma}^\mu(\vec{x}) e^{-i\Omega_m^\Sigma t} + \hat{c}_{am}^{\Sigma\dagger} a_{m\Sigma}^{\mu *}(\vec{x}) e^{i\Omega_m^\Sigma t} \right], \tag{2.45}$$

where m is the set of quantum numbers $m = \{N, J, M\}$ which denote the radial, angular momentum and magnetic quantum numbers respectively. The terms $a_{m\Sigma}^\mu(\vec{x})$ are the gluon cavity modes, the operators $\hat{c}_{am}^{\Sigma\dagger}$ and $\hat{c}_{am}^\Sigma$ are the gluon creation and annihilation operators for a gluon with the quantum numbers a and m and the polarization Σ. The gluon field operator satisfies the commutation relation (2.19) which reduces to the commutation relation of the gluon creation and annihilation operators

$$\left[\hat{c}_{am}^\Sigma, \hat{c}_{a'm'}^{\Sigma'\dagger} \right] = -g^{\Sigma\Sigma'} \delta_{aa'} \delta_{mm'}, \tag{2.46}$$

where $g^{\Sigma\Sigma'}$ is the metric tensor in the polarization space which is defined as

$$g^{\mathcal{SS}} = -g^{\mathcal{LL}} = -g^{\mathcal{MM}} = -g^{\mathcal{EE}} = 1, \tag{2.47}$$

$$g^{\Sigma\Sigma'} = 0 \qquad \text{if} \qquad \Sigma \neq \Sigma',$$

where $\mathcal{S}$ stands for the scalar, $\mathcal{L}$ for the longitudinal, $\mathcal{M}$ for the transverse magnetic, and $\mathcal{E}$ for the transverse electric polarization.

The gluon propagator is the vacuum expectation value of the time-ordered product of the gluon field operators

$$iD_{ab}^{\mu\nu}(x, x') = \left\langle \hat{0} \left| T \left[\hat{A}_\mu(x) \hat{A}_b^\nu(x') \right] \right| \hat{0} \right\rangle. \tag{2.48}$$

Using the gluon field expansion (2.45) and the commutation relation (2.46) one finds

$$iD_{ab}^{\mu\nu}(x, x') = -\delta_{ab} \sum_{m\Sigma} \frac{g^{\Sigma\Sigma}}{2\Omega_m^\Sigma} a_{m\Sigma}^\mu(\vec{x}) a_{m\Sigma}^{\nu *}(\vec{x}') e^{-i\Omega_m^\Sigma |t-t'|} \tag{2.49}$$

or by employing the integral representation of the theta function (2.43)

$$iD_{ab}^{\mu\nu}(x, x') = -i\delta_{ab} \sum_{m\Sigma} g^{\Sigma\Sigma} a_{m\Sigma}^\mu(\vec{x}) a_{m\Sigma}^{\nu *}(\vec{x}') \int \frac{d\omega}{2\pi} \frac{e^{i\omega(t'-t)}}{\omega^2 - (\Omega_m^\Sigma)^2 + i0}. \tag{2.50}$$

This expression is the Feynman propagator of a gluon in cavity QCD using the Feynman gauge, i.e. the gauge parameter λ in Equation (2.1) is set to 1. One can

also write it down in an arbitrary gauge as it has been done by Stoddart [22]. Only gauge-independent graphs are calculated, so this more convenient form of the gluon propagator will be used. The gluon propagator $D^{\mu\nu}_{ab}(x,x')$ satisfies the inhomogeneous d'Alambert equation

$$\Box_x D^{\mu\nu}_{ab}(x,x') = \delta_{ab}\, g^{\mu\nu}\delta^{(4)}(x,x'). \tag{2.51}$$

2.3 The Gell-Mann and Low Theorem

To describe transition amplitudes in cavity QCD. one often uses the energy shift induced by an interaction. For example, in the cases considered here, the one- and two-gluon exchanges between two quarks, the energy shift calculated is the difference in energy between a state containing two non-interacting quarks and the state of two quarks exchanging one or two gluons. These energy shifts are usually calculated via the Gell-Mann and Low theorem [46, 47] which will be briefly reviewed here.

First one needs to introduce the time-evolution operator $U(t,t')$

$$U\left(t,t'\right) = U(t)U^{-1}(t'). \tag{2.52}$$

$U(t,t')$ satisfies the same differential equation as $U(t)$,

$$i\frac{\partial}{\partial t}U(t,t') = U(t,t')\hat{H}_{\rm int} \tag{2.53}$$

and the initial condition $U(t,t) = 1$. The time-evolution operator transports a state in the Dirac picture from the time t' to the time t

$$|\hat{\psi}(t)\rangle = U(t,t')|\hat{\psi}(t')\rangle. \tag{2.54}$$

If one introduces an adiabatic switching on of the interaction Hamiltonian by defining

$$\hat{H}^{\varepsilon}_{\rm int}(t) = e^{-\varepsilon|t|}\hat{H}_{\rm int}(t). \tag{2.55}$$

with $\varepsilon > 0$, then one can write the solution of Equation (2.53) in terms of Dyson's expansion, expressing $U^{\varepsilon}(t,t')$ as a series of time-ordered products of $\hat{H}^{\varepsilon}_{\rm int}(t)$ (cf. the well-known book by Fetter and Walecka [47]),

$$U^{\varepsilon}(t,t') = \sum_{n=0}^{\infty}\frac{(-i)^n}{n!}\int_{t'}^{t}dt_1\cdots\int_{t'}^{t}dt_n T\left[\hat{H}^{\varepsilon}_{\rm int}(t_1)\cdots\hat{H}^{\varepsilon}_{\rm int}(t_n)\right]. \tag{2.56}$$

The Gell-Mann and Low theorem states that if $\{|\hat{\phi}_k\rangle\}$ is a complete and orthonormal set of eigenvectors of the non-interacting Hamiltonian, then

$$|\psi_k\rangle = \lim_{\varepsilon\to 0_+} \frac{U^\varepsilon(0,-\infty)|\hat{\phi}_k\rangle}{\langle\hat{\phi}_k|U^\varepsilon(0,-\infty)|\hat{\phi}_k\rangle} \tag{2.57}$$

is an eigenstate of the full Hamiltonian at $t = 0$ if $|\psi_k\rangle$ exists to all orders. The energy shift between the interacting and non-interacting systems can then be expressed as

$$E_k - E_k^0 = \lim_{\varepsilon\to 0_+} \frac{\langle\hat{\phi}_k|\hat{H}^\varepsilon_{\rm int}U^\varepsilon(0,-\infty)|\hat{\phi}_k\rangle}{\langle\hat{\phi}_k|U^\varepsilon(0,-\infty)|\hat{\phi}_k\rangle}. \tag{2.58}$$

There exists an alternative form of the Gell-Mann and Low theorem due to Sucher [48], which is symmetric in time. Here the energy shift is given by

$$E_k - E_k^0 = \lim_{\substack{\eta\to 1\\ \varepsilon\to 0_+}} \frac{i\varepsilon}{2} \frac{\partial\langle\hat{\phi}_k|S^\varepsilon_\eta|\hat{\phi}_k\rangle_c/\partial\eta}{\langle\hat{\phi}_k|S^\varepsilon_\eta|\hat{\phi}_k\rangle_c}, \tag{2.59}$$

where the subscript c means that only the connected diagrams are included. S^ε_η is the adiabatic S-matrix and can be written as

$$S^\varepsilon_\eta = 1 + \sum_{n=1}^{\infty} S^{\varepsilon(n)}_\eta \tag{2.60}$$

with

$$S^{\varepsilon(n)}_\eta = \frac{(i\eta)^n}{n!}\int_{-\infty}^{\infty} dt_1 \cdots \int_{-\infty}^{\infty} dt_n T\left[\hat{H}^\varepsilon_{\rm int}(t_1)\cdots\hat{H}^\varepsilon_{\rm int}(t_n)\right]. \tag{2.61}$$

The advantage of this form is that one does not need to decompose the Feynman diagrams into time-ordered diagrams due to the time-symmetric integration limits. However, the time integrations become more complicated, since the energy denominators have to be calculated.

One can expand the energy shift in terms of the $S^{\varepsilon(n)}$ by substituting (2.60) into Equation (2.59) and taking the limit $\eta \to 1$. Only terms up to order four in g are kept since only diagrams up to order α_S^2 are calculated in this thesis. One obtains

$$\Delta E = \lim_{\varepsilon\to 0_+} \frac{i\varepsilon}{2} \frac{\langle S^{(1)}\rangle_c + 2\langle S^{(2)}\rangle_c + 3\langle S^{(3)}\rangle_c + 4\langle S^{(4)}\rangle_c + \cdots}{1 + \langle S^{(1)}\rangle_c + \langle S^{(2)}\rangle_c + \langle S^{(3)}\rangle_c + \langle S^{(4)}\rangle_c + \cdots}. \tag{2.62}$$

Using the expansion $1/(1+x) = 1 - x + x^2 \cdots$ one finds that the energy shift up to order $\mathcal{O}(g^4)$ can be written as

$$\begin{aligned}\Delta E = \lim_{\varepsilon\to 0_+} \frac{i\varepsilon}{2} \quad & \Big[\langle S^{(1)}\rangle_c + 2\langle S^{(2)}\rangle_c - \langle S^{(1)}\rangle_c^2 \\ & + 3\langle S^{(3)}\rangle_c + \langle S^{(1)}\rangle_c^3 - 3\langle S^{(1)}\rangle_c\langle S^{(2)}\rangle_c \\ & + 4\langle S^{(4)}\rangle_c - \langle S^{(1)}\rangle_c^4 + 2\langle S^{(1)}\rangle_c^2\langle S^{(2)}\rangle_c \\ & + \langle S^{(1)}\rangle_c\langle S^{(3)}\rangle_c - 2\langle S^{(2)}\rangle_c^2\Big].\end{aligned} \tag{2.63}$$

Only the terms of even order in g are connected to the asymptotic states of hadrons dealt with in this thesis, so the energy shift is

$$\Delta E = \lim_{\varepsilon \to 0_+} \frac{i\varepsilon}{2} \quad \Big[2\langle S^{(2)} \rangle_c + 4\langle S^{(4)} \rangle_c - \langle S^{(1)} \rangle_c^2 - \langle S^{(1)} \rangle_c^4 + 2\langle S^{(1)} \rangle_c^2 \langle S^{(2)} \rangle_c + \langle S^{(1)} \rangle_c \langle S^{(3)} \rangle_c - 2\langle S^{(2)} \rangle_c^2 \Big] . \tag{2.64}$$

The first term gives the second order contribution in g, the second term the fourth order contribution. The remaining terms are responsible for cancelling the poles in the Feynman diagrams. The work in this thesis concentrates on evaluating the non-divergent parts of the first two terms.

Chapter 3

Cavity Calculations

The energy shift due to the the non-divergent Feynman diagrams up to order α_S^2 can be calculated by evaluating Equation (2.64). Only the quark-gluon coupling of the interaction Hamiltonian are considered here, since all other terms are either of different order or not connected to the asymptotic states consisting of two or three quarks. One can thus write

$$H_{\text{int}}(t) = -\int d^3x\, \bar{\psi}(x) g \frac{\lambda_a}{2} \not{A}_a(x) \psi(x). \tag{3.1}$$

Since only the non-divergent diagrams are considered, there are just three possible interactions between two quarks: the one-gluon exchange and the two topologically distinct two-gluon exchanges. As an introductory example, the one-gluon exchange is considered first.

3.1 The One-Gluon Exchange Diagram

The simplest term contributing to the energy shift up to order α_S is the first term of Equation (2.64), which contains the one-gluon exchange diagram. The quark self-energy is also contained in this term, but since it is divergent, it is not calculated here. It is

$$\Delta E = \lim_{\varepsilon \to 0_+} i\varepsilon \langle S_\varepsilon^{(2)} \rangle_c. \tag{3.2}$$

The corresponding Feynman diagram for the one-gluon exchange is given in Figure 3.1. If the interaction Hamiltonian (3.1) is substituted into the expression for $\langle S_\varepsilon^{(2)} \rangle_c$,

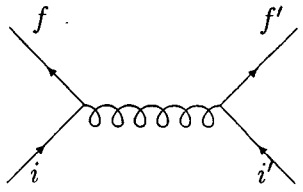

Figure 3.1: *The one-gluon exchange diagram. The labels on the incoming and outgoing quarks represent all the quantum numbers of these fields.*

Equation (2.61), one obtains

$$\begin{aligned}\Delta E &= \lim_{\varepsilon\to 0_+} i\varepsilon\frac{(-i)^2}{2!}\int d^4x_1\int d^4x_2\, e^{-\varepsilon(|t_1|+|t_2|)} \\ &\quad\times\left\langle\hat{X}\left|T\left[\left(\hat{\bar{\psi}}g\frac{\lambda_a}{2}\hat{\not{A}}_a\hat{\psi}\right)_{x_1}\left(\hat{\bar{\psi}}g\frac{\lambda_b}{2}\hat{\not{A}}_b\hat{\psi}\right)_{x_2}\right]\right|\hat{X}\right\rangle,\end{aligned} \tag{3.3}$$

where $|\hat{X}\rangle$ is an asymptotic state, an eigenvector of the non-interacting Hamiltonian representing a hadron state. For baryons, the state $|\hat{X}\rangle$ can be written as a linear combination of three quark creation operators acting on the vacuum:

$$|\hat{X}\rangle \sim a^\dagger_{c_1 f_1 n_1} a^\dagger_{c_2 f_2 n_2} a^\dagger_{c_3 f_3 n_3}|\hat{0}\rangle. \tag{3.4}$$

The time-ordered product can be expressed as the normal ordered product of the sum of all possible contractions connected to the asymptotic states. This is known as Wick's theorem [47]. The contractions of the field operators are just the field propagators given in Section 2.2. Here only the one-gluon exchange shown in Figure 3.1 is considered. It can be expressed as

$$\begin{aligned}\Delta E &= -\lim_{\varepsilon\to 0}\frac{i\varepsilon}{2}g^2\int d^4x_1\int d^4x_2\, e^{-\varepsilon(|t_1|+|t_2|)} \\ &\quad\times\left\langle\hat{X}\left|T\left[\left(\hat{\bar{\psi}}g\tfrac{\lambda_a}{2}\hat{\not{A}}_a\hat{\psi}\right)_{x_1}\left(\hat{\bar{\psi}}g\tfrac{\lambda_b}{2}\hat{\not{A}}_b\hat{\psi}\right)_{x_2}\right]\right|\hat{X}\right\rangle.\end{aligned} \tag{3.5}$$

Substituting the cavity-mode expansion of the quark fields and of the gluon propagator yields

$$\Delta E = -\lim_{\varepsilon\to 0_+}\frac{i\varepsilon}{2}g^2\left\langle\hat{X}\left|a^\dagger_{c'f'\alpha'}a^\dagger_{d'g'\beta'}\left(\frac{\lambda_a}{2}\right)_{c'c}\left(\frac{\lambda_a}{2}\right)_{d'd}a_{dg\beta}a_{cf\alpha}\right|\hat{X}\right\rangle$$

$$\times \sum_{m\Sigma} \frac{g^{\Sigma\Sigma}}{2\Omega_m^\Sigma} Q_{fi}^{m\Sigma} \tilde{Q}_{f'i'}^{m\Sigma}$$
$$\times \int dt_1 dt_2 \, e^{-\varepsilon(|t_1|+|t_2|)} e^{it_1(\varepsilon_f - \varepsilon_i)} e^{it_2(\varepsilon_{f'} - \varepsilon_{i'})} e^{-i\Omega_m^\Sigma |t_1 - t_2|}, \tag{3.6}$$

where the $Q_{n'n}^{m\Sigma}$ are the quark-gluon vertex integrals as defined in Appendix B. The remaining integrals can be solved,

$$\lim_{\varepsilon \to 0_+} i\varepsilon \int dt_1 dt_2 \, e^{-\varepsilon(|t_1|+|t_2|)} e^{it_1(\varepsilon_f - \varepsilon_i)} e^{it_2(\varepsilon_{f'} - \varepsilon_{i'})} e^{-i\Omega_m^\Sigma |t_1 - t_2|}$$
$$= \delta(\varepsilon_f - \varepsilon_i + \varepsilon_{f'} - \varepsilon_{i'}) \left(\frac{1}{\varepsilon_{f'} - \varepsilon_{i'} + \Omega_m^\Sigma} + \frac{1}{\varepsilon_f - \varepsilon_i + \Omega_m^\Sigma} \right) \tag{3.7}$$
$$= \frac{2}{\Omega_m^\Sigma} \qquad \text{for} \quad \varepsilon_i = \varepsilon_{i'} \quad \text{and} \quad \varepsilon_f = \varepsilon_{f'}. \tag{3.8}$$

The two terms in Equation (3.7) show how the two different possible time-ordered graphs can be extracted from the Feynman diagram by performing the symmetric time-integration. The same process will be used in the second order case, only there one will obtain 24 energy denominators.

Since only contractions connected to quarks in the lowest cavity modes contribute to the energy shift in baryons, Equation (3.8) can be inserted into Equation (3.6). One obtains

$$\Delta E = -g^2 \left\langle \hat{C}^{(2)} \right\rangle \sum_{m\Sigma} \frac{g^{\Sigma\Sigma}}{(\Omega_m^\Sigma)^2} Q_{fi}^{m\Sigma} \tilde{Q}_{f'i'}^{m\Sigma}, \tag{3.9}$$

where

$$\left\langle \hat{C}^{(2)} \right\rangle = \left\langle \hat{X} \left| a_{c'f'\alpha'}^\dagger a_{d'g'\beta'}^\dagger \left(\frac{\lambda_a}{2} \right)_{c'c} \left(\frac{\lambda_a}{2} \right)_{d'd} a_{dg\beta} a_{cf\alpha} \right| \hat{X} \right\rangle \tag{3.10}$$

are the colour flavour matrix elements. Thus, ΔE can be interpreted as a two-body operator $\hat{V}$ sandwiched between the state $|\hat{X}\rangle$, where

$$\hat{V} = -g^2 \left(\frac{\lambda_a}{2} \right)_{c'c} \left(\frac{\lambda_a}{2} \right)_{d'd} \frac{g^{\Sigma\Sigma}}{(\Omega_m^\Sigma)^2} Q_{fi}^{m\Sigma} \tilde{Q}_{f'i'}^{m\Sigma} a_{c'f'\alpha'}^\dagger a_{d'g'\beta'}^\dagger a_{dg\beta} a_{cf\alpha}. \tag{3.11}$$

To describe a complex many-quark system, it is convenient to have the two-body operator, Equation (3.11) in first instead of second quantization. The two-body operator V_{12} corresponding to $\hat{V}$ can be written in the form

$$V_{12} = \frac{\alpha_S}{R} \boldsymbol{F}_1 \cdot \boldsymbol{F}_2 \sum_J \mu_{12}(J) K_{12}(J), \tag{3.12}$$

where J is the angular momentum exchanged between the quarks and $\boldsymbol{F}_i$, $i = 1, 2$, denotes the colour generator in the fundamental representation.

The operators $\mu_{12}(J)$ and $K_{12}(J)$ operate on the radial and angular part of the two-body wave function respectively. In Appendix B, it has been shown how the quark-gluon vertex integrals can be separated into radial and angular momentum parts. One can write $\mu_{12}(J)$ and $K_{12}(J)$ as

$$\langle f, f'|\mu_{12}(J)|i, i'\rangle = -\sum_{\Sigma N} \frac{\eta_\Sigma g^{\Sigma\Sigma}}{(2J+1)(\Omega_\Sigma^m R)^2} S_{fi}^{\Sigma m} S_{f'i'}^{\Sigma m}, \tag{3.13}$$

where

$$S_{fi}^{\Sigma m} = \frac{(1 - \eta_\Sigma g^{\Sigma\Sigma}(-1)^{l_f+J+l_i})}{2} R_{fi}^{\Sigma m} \tag{3.14}$$

and

$$\langle f, f'|K_{12}(J)|i, i'\rangle = (2J+1) \sum_{M=-J}^{J} (-1)^M F_{JM}(f, i) F_{J-M}(f', i'), \tag{3.15}$$

where

$$F_{JM}(f, i) = (-1)^{\mu_f + 1/2} \hat{j}\hat{J}\hat{j}' \begin{pmatrix} j_f & J & j_i \\ \frac{1}{2} & 0 & -\frac{1}{2} \end{pmatrix} \begin{pmatrix} j_f & J & j_i \\ -\mu_f & M & \mu_i \end{pmatrix}. \tag{3.16}$$

If one considers only hadrons consisting of quarks or antiquarks in their ground state, i.e. $j = \frac{1}{2}$, one can write $\hat{V}$ explicitly and obtain both $\mu_{12}(J)$ and $K_{12}(J)$. One uses the definition of the one-body spin operator $\boldsymbol{S}$, which is in spherical coordinates given by

$$(S^k)_{m'm} = (-1)^{m'-1/2} \sqrt{\frac{3}{2}} \begin{pmatrix} \frac{1}{2} & 1 & \frac{1}{2} \\ -m' & k & m \end{pmatrix}. \tag{3.17}$$

The scalar product in spherical coordinates is defined as

$$\boldsymbol{S}_1 \cdot \boldsymbol{S}_2 = \sum_{k=-1}^{1} (-1)^k S_1^k S_2^{-k}. \tag{3.18}$$

Then it is easily shown that

$$K(0) = 1 \tag{3.19}$$

$$K(1) = 4\, \boldsymbol{S}_1 \cdot \boldsymbol{S}_2. \tag{3.20}$$

$\boldsymbol{S}_1 \cdot \boldsymbol{S}_2$ is found using the fact that

$$(\boldsymbol{S}_1 + \boldsymbol{S}_2)^2 = \boldsymbol{S}_1^2 + 2\, \boldsymbol{S}_1 \cdot \boldsymbol{S}_2 + \boldsymbol{S}_2^2 = J(J+1). \tag{3.21}$$

So for a two quark-system

$$\boldsymbol{S}_1 \cdot \boldsymbol{S}_2 = \frac{1}{2}\left(J(J+1) - \frac{3}{2}\right). \tag{3.22}$$

The $\mu_{12}(J)$ have to be calculated numerically. For this diagram, these calculations are short and quite easily done once the numerical routines described in Appendix C are set up. This is so, because the parity conservation terms in Equation (3.13), $(1 - \eta_\Sigma\, g^{\Sigma\Sigma}(-1)^{l_f+J+j_i})/2$, together with the condition $j_n = \frac{1}{2}$ for the external quark states, allow only for $J = 0$ or $J = 1$. $J = 0$ is only possible for $\Sigma = \mathcal{S}, \mathcal{L}$ and $J = 1$ for $\Sigma = \mathcal{M}$. The sum over the internal states reduces therefore to a sum over only the radial quantum numbers N of the gluon.

$$\mu_{12}(0) = \sum_{\Sigma=\mathcal{S},\mathcal{L}} \sum_N \frac{1}{(\Omega_m^\Sigma R)^2} R_{fi}^{\{N,0,0\}\Sigma} R_{f'i'}^{\{N,0,0\}\Sigma} \tag{3.23}$$

$$\mu_{12}(1) = -\sum_N \frac{1}{3(\Omega_m^\Sigma R)^2} R_{fi}^{\{N,1,M\}\mathcal{M}} R_{f'i'}^{\{N,1,M\}\mathcal{M}} \tag{3.24}$$

Numerical evaluation of $\mu_{12}(J)$ for two massless quarks yields

$$\begin{aligned} \mu_{12}(0) &= 0.00980 \\ \mu_{12}(1) &= -0.17702 \end{aligned} \tag{3.25}$$

so that finally V_{12} can be written as

$$V_{12} = \frac{\alpha_S}{R} \boldsymbol{F}_1 \cdot \boldsymbol{F}_2 (0.00980 - 0.70808 \boldsymbol{S}_1 \cdot \boldsymbol{S}_2). \tag{3.26}$$

The values are in excellent agreement with the results from e.g. Buser *et al.* [21]. One also needs to find the two-body operator for a two-body system containing one or two massive quarks. These results will be listed at the end of this chapter, combined with the results of the two-gluon exchange Feynman diagrams. With this check of the numerical routines passed, more complicated calculations can now be tackled.

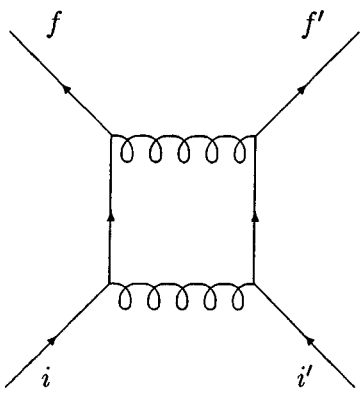

Figure 3.2: *Straight two-gluon exchange diagram.*

3.2 The Two-Gluon Exchange Diagrams

The energy shift due to quark-gluon interactions of order g^4 is given by

$$\Delta E = \lim_{\varepsilon \to 0_+} 2i\varepsilon \frac{(-i)^4}{4!} g^4 \int d^4x_1\, d^4x_2\, d^4x_3\, d^4x_4\, e^{-\varepsilon(|t_1|+|t_2|+|t_3|+|t_4|)}$$
$$\times \left\langle \hat{X} \left| T \left[\left(\hat{\bar{\psi}} g \frac{\lambda_a}{2} \hat{\not{A}}_a \hat{\psi} \right)_{x_1} \left(\hat{\bar{\psi}} g \frac{\lambda_b}{2} \hat{\not{A}}_b \hat{\psi} \right)_{x_2} \left(\hat{\bar{\psi}} g \frac{\lambda_c}{2} \hat{\not{A}}_c \hat{\psi} \right)_{x_3} \left(\hat{\bar{\psi}} g \frac{\lambda_d}{2} \hat{\not{A}}_d \hat{\psi} \right)_{x_4} \right] \right| \hat{X} \right\rangle . \tag{3.27}$$

There are two possible structures of contractions connected to two free quark fields. They yield the two topologically distinct Feynman diagrams in Figures 3.2 and 3.3. Due to their appearance they are called "straight" and "crossed" two-gluon exchange diagrams. For these two second-order interactions one can also find a two-body operator as in the first-order case above. However, the calculations are more difficult, since one first has to combine the two-gluon transfers into one apparent interaction. One also has to sum over four internal states now, which lead to very lengthy (especially in time) numerical calculations.

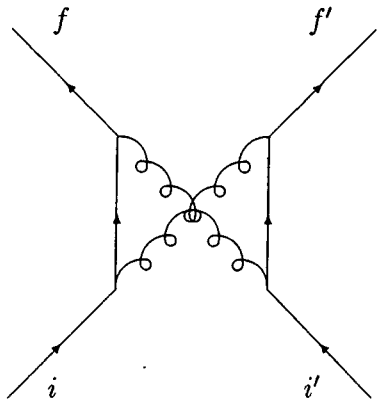

Figure 3.3: *Crossed two-gluon exchange diagram.*

3.2.1 The "Straight" Two-Gluon Exchange Diagram

The diagram for the straight two-gluon exchange is obtained by considering the contractions

$$\Delta E = \lim_{\varepsilon \to 0_+} 2i\varepsilon g^4 \int d^4x_1\, d^4x_2\, d^4x_3\, d^4x_4\, e^{-\varepsilon(|t_1|+|t_2|+|t_3|+|t_4|)} \times \left\langle \hat{X} \left| T \left[\left(\hat{\bar{\psi}} g \frac{\lambda_a}{2} \hat{\not{A}}_a \hat{\psi} \right)_{x_1} \left(\hat{\bar{\psi}} g \frac{\lambda_b}{2} \hat{\not{A}}_b \hat{\psi} \right)_{x_2} \left(\hat{\bar{\psi}} g \frac{\lambda_c}{2} \hat{\not{A}}_c \hat{\psi} \right)_{x_3} \left(\hat{\bar{\psi}} g \frac{\lambda_d}{2} \hat{\not{A}}_d \hat{\psi} \right)_{x_4} \right] \right| \hat{X} \right\rangle , \tag{3.28}$$

where a factor of 4! has already been included. It arises due to the symmetry in the integration over all for space-time points x_i. Inserting the quark fields and the quark and gluon propagators in terms of cavity modes yields 24 terms which are distinct in their time order. Each contains an integral of the form

$$\lim_{\varepsilon \to 0_+} i\varepsilon \int_{-\infty}^{\infty} dt_1 \int_{-\infty}^{t_1} dt_2 \int_{-\infty}^{t_2} dt_3 \int_{-\infty}^{t_3} dt_4\, e^{-\varepsilon(|t_1|+|t_2|+|t_3|+|t_4|)} e^{it_1 w} e^{it_2 x} e^{it_3 y} e^{it_4 z} \tag{3.29}$$

which can be evaluated to equal

$$-\frac{\delta(w+x+y+z)}{2z(y+z)(x+y+z)} \tag{3.30}$$

if one excludes all the divergent terms. Only the term $y+z$ can become zero, all the others are of the form $(-\varepsilon_f + \varepsilon_q + \Omega_m^{\Sigma})$ which cannot become zero. The divergent terms can be excluded, since they are cancelled by some of the composite

contributions to ΔE, eg. $\langle S^{(1)}\rangle_c\langle S^{(3)}\rangle_c$. The result is

$$\Delta E = -g^4 \left\langle \hat{X} \left| a^\dagger_{c'mf} a^\dagger_{d'nf'} \left(\frac{\lambda_a}{2}\right)_{c'j} \left(\frac{\lambda_a}{2}\right)_{d'k} \left(\frac{\lambda_b}{2}\right)_{jc} \left(\frac{\lambda_b}{2}\right)_{kd} a_{dni'} a_{cmi} \right| \hat{X} \right\rangle \times \delta(\varepsilon_i + \varepsilon_{i'} - \varepsilon_f - \varepsilon_{f'}) \sum_{\Sigma\Sigma'} \sum_{qq'} \sum_{mm'} \frac{g^{\Sigma\Sigma} g^{\Sigma'\Sigma'}}{4\,\Omega^\Sigma_m\,\Omega^{\Sigma'}_{m'}}\, \mathcal{Q}_S. \tag{3.31}$$

The subscripts of the quark creation and annihilation operators stand for the colour, flavour, and all other quantum numbers respectively. Repeated indices on the Gell-Mann matrices indicate a summation according to the Einstein sum convention. All the quark-gluon vertex integrals are combined into the function $\mathcal{Q}_S$ which depends on all the quark and gluon quantum numbers involved in the process. Because there are too many to be explicitly given, they are suppressed.

$$\begin{aligned} \mathcal{Q}_S = {} & Q^{m\Sigma}_{fq} Q^{m\Sigma}_{f'q'} Q^{m'\Sigma'}_{qi} Q^{m'\Sigma'}_{q'i'} E_{\rm I} - Q^{m\Sigma}_{fq} Q^{m\Sigma}_{f'-q'} Q^{m'\Sigma'}_{qi} Q^{m'\Sigma'}_{-q'i'} E_{\rm II} \\ & - Q^{m\Sigma}_{f-q} Q^{m\Sigma}_{f'q'} Q^{m'\Sigma'}_{-qi} Q^{m'\Sigma'}_{q'i'} E_{\rm III} + Q^{m\Sigma}_{f-q} Q^{m\Sigma}_{f'-q'} Q^{m'\Sigma'}_{-qi} Q^{m'\Sigma'}_{-q'i'} E_{\rm IV}. \end{aligned} \tag{3.32}$$

The terms $E_{\rm I}$–$E_{\rm IV}$ are sums over the energy denominators that arise from the time integrations. They are given for this diagram in Appendix D.1. These terms are shown in the form of Feynman diagrams in Figure 3.4. If one replaces q with q' and m with m' in term III, one ends up with term II again. This symmetry is clearly seen in the diagrams. One therefore only has to calculate numerical values for I, II, and IV. This is obviously only true for the interaction of two either massless or massive quarks. If one considers the interaction of a massive and a massless quark, one has to calculate all four terms.

As in the case of the one-gluon exchange, the energy shift can be interpreted as a two-body operator $\hat{W}^{\mathcal{S}}$ sandwiched between the state $|\hat{X}\rangle$. Using the identity

$$\left(\frac{\lambda_a}{2}\right)_{c'c} \left(\frac{\lambda_a}{2}\right)_{d'd} = \frac{1}{2}\left(\delta_{c'd}\delta_{cd'} - \frac{1}{3}\delta_{cc'}\delta_{dd'}\right) \tag{3.33}$$

twice, one finds that this operator can be written in the form

$$W^{\mathcal{S}}_{12} = \frac{\alpha_S^2}{R} (\boldsymbol{F}_1 \cdot \boldsymbol{F}_2)^2 \sum_\Lambda \nu^{\mathcal{S}}_{12}(\Lambda), \tag{3.34}$$

where Λ stands for the total exchanged angular momentum between the quarks. Unfortunately, one cannot break the terms depending on Λ, into radial and angular

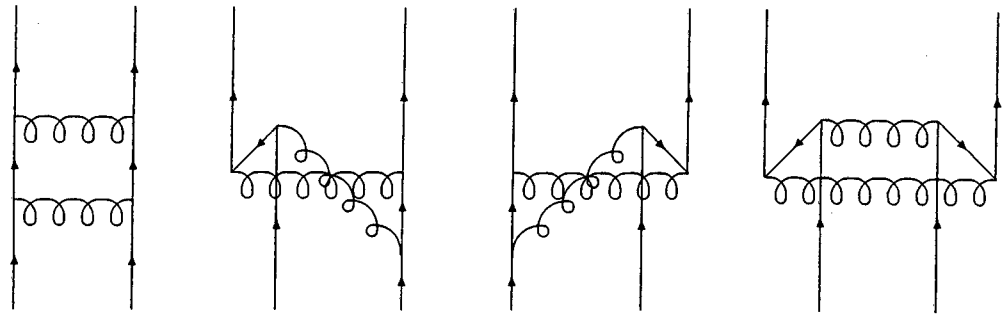

Figure 3.4: *These four diagrams represent the four terms in Equation (3.32). In this graphical representation one can clearly see the symmetry between the terms II and III for two identical interacting particles.*

momentum parts, since one has to sum internally over the total angular momenta J_1 and J_2 carried by each of the gluons.

After expanding the quark-gluon vertex integrals into angular and radial parts, one can evaluate the sum over the spin quantum numbers of the internal quark- and gluon-fields. This introduces 6j-symbols and the total transferred angular momentum Λ mentioned above. The necessary relations are given in Section C.4. One finally obtains

$$\begin{aligned}
\nu_{12}^{\mathcal{S}}(\Lambda) \;=\; & -\sum_{\Sigma\Sigma'}\sum_{j_q j_{q'}}\sum_{J_1 J_2}\sum_{\lambda}\frac{g^{\Sigma\Sigma}\eta_{\Sigma}\, g^{\Sigma'\Sigma'}\eta_{\Sigma'}}{4\,\Omega_m^{\Sigma} R\,\Omega_{m'}^{\Sigma'} R}(-1)^{J_1+J_2+\Lambda} \\
& \times G_{J_1J_2}(f,q,i)\, G_{J_1J_2}(f',q',i')\,\hat{\Lambda}^2 \begin{Bmatrix} j_f & J_1 & j_q \\ J_2 & j_i & \Lambda \end{Bmatrix} \begin{Bmatrix} j_{f'} & J_1 & j_{q'} \\ J_2 & j_{i'} & \Lambda \end{Bmatrix} \\
& \times (-1)^{1+\mu_{f'}-\mu_i} \begin{pmatrix} j_f & \Lambda & j_i \\ -\mu_f & \lambda & \mu_i \end{pmatrix} \begin{pmatrix} j_{f'} & \Lambda & j_{i'} \\ -\mu_{f'} & -\lambda & \mu_{i'} \end{pmatrix} \frac{\mathcal{S}}{R^3}, \qquad (3.35)
\end{aligned}$$

where the functions G and $\mathcal{S}$ have been introduced to shorten the notation. The summation over the radial quantum numbers of the intermediate quarks and gluons have also been omitted. G and $\mathcal{S}$ are defined as:

$$G_{J_1J_2}(f,q,i) = \hat{j}_f\,\hat{j}_i\,\hat{j}_q^2\,\hat{J}_1\hat{J}_2\,(-1)^{j_f+j_i-j_q} \begin{pmatrix} j_f & J_1 & j_q \\ \frac{1}{2} & 0 & -\frac{1}{2} \end{pmatrix} \begin{pmatrix} j_q & J_2 & j_i \\ \frac{1}{2} & 0 & -\frac{1}{2} \end{pmatrix} \qquad (3.36)$$

and

$$\begin{aligned}\mathcal{S} \;=\;& S^{m\Sigma}_{fq}\,S^{m\Sigma}_{f'q'}\,S^{m'\Sigma'}_{qi}\,S^{m'\Sigma'}_{q'i'}\,E_{\rm I} \;-\; S^{m\Sigma}_{fq}\,S^{m\Sigma}_{f'-q'}\,S^{m'\Sigma'}_{qi}\,S^{m'\Sigma'}_{-q'i'}\,E_{\rm II}\\ -\;& S^{m\Sigma}_{f-q}\,S^{m\Sigma}_{f'q'}\,S^{m'\Sigma'}_{-qi}\,S^{m'\Sigma'}_{q'i'}\,E_{\rm III} \;+\; S^{m\Sigma}_{f-q}\,S^{m\Sigma}_{f'-q'}\,S^{m'\Sigma'}_{-qi}\,S^{m'\Sigma'}_{-q'i'}\,E_{\rm IV}.\end{aligned} \tag{3.37}$$

For $j_n = \frac{1}{2}$ with $n = i, i', f, f'$, Equation (3.35) simplifies enormously and the same structure as in Equation (3.26) emerges, since the 3j-symbols only allow $\Lambda = 0, 1$. One finds

$$\begin{aligned}\nu^{\mathcal{S}}_{12}(0) \;=\;& -\sum_{\Sigma\Sigma'}\sum_{J j_q j_{q'}} \frac{g^{\Sigma\Sigma}\eta_\Sigma\, g^{\Sigma'\Sigma'}\eta_{\Sigma'}}{4\,\Omega^{\Sigma}_{m} R\,\Omega^{\Sigma'}_{m'} R}\hat{j}_q^2\,\hat{j}_{q'}^2\,\hat{J}^2\,\delta_{J_1 J_2}\begin{pmatrix}\frac{1}{2} & J & j_q\\ \frac{1}{2} & 0 & -\frac{1}{2}\end{pmatrix}^2\\ &\times\begin{pmatrix}\frac{1}{2} & J & j_{q'}\\ \frac{1}{2} & 0 & -\frac{1}{2}\end{pmatrix}^2\frac{\mathcal{S}}{R^3},\end{aligned} \tag{3.38}$$

$$\begin{aligned}\nu^{\mathcal{S}}_{12}(1) \;=\;& -8\,\boldsymbol{S}_1\cdot\boldsymbol{S}_2\sum_{\Sigma\Sigma'}\sum_{J_1 J_2 j_q j_{q'}}\frac{g^{\Sigma\Sigma}\eta_\Sigma\, g^{\Sigma'\Sigma'}\eta_{\Sigma'}}{4\,\Omega^{\Sigma}_{m} R\,\Omega^{\Sigma'}_{m'} R}(-1)^{J_1+J_2-j_q-j_{q'}}\,\hat{j}_q^2\,\hat{j}_{q'}^2\,\hat{J}_1^2\,\hat{J}_2^2\\ &\times\begin{Bmatrix}\frac{1}{2} & J_1 & j_q\\ J_2 & \frac{1}{2} & 1\end{Bmatrix}\begin{Bmatrix}\frac{1}{2} & J_1 & j_{q'}\\ J_2 & \frac{1}{2} & 1\end{Bmatrix}\begin{pmatrix}\frac{1}{2} & J_1 & j_q\\ \frac{1}{2} & 0 & -\frac{1}{2}\end{pmatrix}\\ &\times\begin{pmatrix}j_q & J_2 & \frac{1}{2}\\ \frac{1}{2} & 0 & -\frac{1}{2}\end{pmatrix}\begin{pmatrix}\frac{1}{2} & J_1 & j_{q'}\\ \frac{1}{2} & 0 & -\frac{1}{2}\end{pmatrix}\begin{pmatrix}j_{q'} & J_2 & \frac{1}{2}\\ \frac{1}{2} & 0 & -\frac{1}{2}\end{pmatrix}\frac{\mathcal{S}}{R^3}.\end{aligned} \tag{3.39}$$

Now one can proceed to the numerical calculations of ν_{12}. This is done by splitting $\nu_{12}(0)$ and $\nu_{12}(1)$ into four parts according to Equation (3.37). They differ merely in the sign of the quantum numbers of the intermediate quarks q and q'. As was noted before q stands for all quantum numbers $\{\nu, \kappa, \mu\}$. Since the sum over μ has already been evaluated and the sum over κ covers both positive and negative values of κ, the different sign only makes a difference for the radial quantum number ν while all conditions derived from parity and angular momentum conservation are the same for the four terms.

For $\nu_{12}(0)$ one finds from the parity conservation factors

$$\frac{(1-\eta_\Sigma g^{\Sigma\Sigma}(-1)^{J+l_q})}{2}\;\frac{(1-\eta_\Sigma g^{\Sigma\Sigma}(-1)^{J+l'_q})}{2}\;\frac{(1-\eta_{\Sigma'} g^{\Sigma'\Sigma'}(-1)^{J+l_q})}{2}\;\frac{(1-\eta_{\Sigma'} g^{\Sigma'\Sigma'}(-1)^{J+l'_q})}{2} \tag{3.40}$$

that $l_q + l_{q'}$ must be even and $\Sigma \neq \mathcal{M} \neq \Sigma'$ or $\Sigma = \mathcal{M} = \Sigma'$. Furthermore, for $\Sigma \neq \mathcal{M}$, one has $J + l_q$ even and for $\Sigma = \mathcal{M}$, $J + l_q$ odd. From angular momentum

conservation in the 3j-symbols, one finds that

$$\left|\max\{j_q, j_{q'}\} - \frac{1}{2}\right| \leq J \leq \min\{j_q, j_{q'}\} + \frac{1}{2}. \tag{3.41}$$

With all these conditions in place the sums are performed in the order Σ, Σ', κ_q, $\kappa_{q'}$, J, ν_q, $\nu_{q'}$, N, N' from the outer to the inner sum.

For massless quarks one finds:

	$\nu_{12}(0)^S$
I	- 0.3637
II, III	0.0137
IV	- 0.0680

(3.42)

Starting with the parity conservation factors of Equation (3.39), one can derive similar conditions for the angular momentum quantum numbers of the intermediate particles for $\nu_{12}(1)$. One sees at once that $l_q + l_{q'}$ is even and thus the following conditions on the angular momentum quantum numbers of the gluons are derived:

Σ	Σ'	l_q even		l_q odd	
$\neq \mathcal{M}$	$\neq \mathcal{M}$	J_1 even	J_2 even	J_1 odd	J_2 odd
$\neq \mathcal{M}$	$= \mathcal{M}$	J_1 even	J_2 odd	J_1 odd	J_2 even
$= \mathcal{M}$	$\neq \mathcal{M}$	J_1 odd	J_2 even	J_1 even	J_2 odd
$= \mathcal{M}$	$= \mathcal{M}$	J_1 odd	J_2 odd	J_1 even	J_2 even

(3.43)

From angular momentum conservation one gets that

$$\left|\max\{j_q, j_{q'}\} - \frac{1}{2}\right| \leq J_1, J_2 \leq \min\{j_q, j_{q'}\} + \frac{1}{2}. \tag{3.44}$$

The sums are performed in the order Σ, Σ', κ_q, $\kappa_{q'}$, J_1, J_2, ν_q, $\nu_{q'}$, N, N'.

For massless quarks (antiquarks) one finally obtains:

	$\nu_{12}^S(1)$
I	0.5437 $S_1 \cdot S_2$
II, III	- 0.0016 $S_1 \cdot S_2$
IV	0.1874 $S_1 \cdot S_2$

(3.45)

The results for massive quarks are listed at the end of the chapter.

3.2.2 The "Crossed" Two-Gluon Exchange Diagram

The diagram for the crossed two-gluon exchange is calculated by evaluating the contractions

$$\Delta E = \lim_{\varepsilon\to 0_+} 2i\varepsilon g^4 \int d^4x_1\, d^4x_2\, d^4x_3\, d^4x_4\, e^{-\varepsilon(|t_1|+|t_2|+|t_3|+|t_4|)} \times \left\langle \hat{X} \left| T\left[\left(\hat{\bar{\psi}} g \frac{\lambda_a}{2} \hat{A}_a \hat{\psi}\right)_{x_1} \left(\hat{\bar{\psi}} g \frac{\lambda_b}{2} \hat{A}_b \hat{\psi}\right)_{x_2} \left(\hat{\bar{\psi}} g \frac{\lambda_c}{2} \hat{A}_c \hat{\psi}\right)_{x_3} \left(\hat{\bar{\psi}} g \frac{\lambda_d}{2} \hat{A}_d \hat{\psi}\right)_{x_4} \right] \right| \hat{X} \right\rangle, \tag{3.46}$$

where, as in the previous section, a factor of 4! has been included for symmetry reasons. This graph can now be evaluated in the same manner as the straight graph.

The energy shift is thus given in second quantization by

$$\Delta E = -g^4 \left\langle \hat{X} \left| a^\dagger_{c'mf} a^\dagger_{d'nf'} \left(\frac{\lambda_a}{2}\right)_{c'j} \left(\frac{\lambda_a}{2}\right)_{kd} \left(\frac{\lambda_b}{2}\right)_{jc} \left(\frac{\lambda_b}{2}\right)_{d'k} a_{dni'} a_{cmi} \right| \hat{X} \right\rangle \times \delta(\varepsilon_i + \varepsilon_{i'} - \varepsilon_f - \varepsilon_{f'}) \sum_{\Sigma\Sigma'} \sum_{qq'} \sum_{mm'} \frac{g^{\Sigma\Sigma} g^{\Sigma'\Sigma'}}{4\,\Omega^\Sigma_m\, \Omega^{\Sigma'}_{m'}}\, \mathcal{Q}_{\rm C}, \tag{3.47}$$

where the function $\mathcal{Q}_{\rm C}$ combines all the quark-gluon vertex integrals for the crossed diagram. It is

$$\begin{aligned} \mathcal{Q}_{\rm C} = {} & Q^{m\Sigma}_{fq} Q^{m\Sigma}_{q'i'} Q^{m'\Sigma'}_{qi} Q^{m'\Sigma'}_{f'q'} E_{\rm I} - Q^{m\Sigma}_{fq} Q^{m\Sigma}_{-q'i'} Q^{m'\Sigma'}_{qi} Q^{m'\Sigma'}_{f'-q'} E_{\rm II} \\ & - Q^{m\Sigma}_{f-q} Q^{m\Sigma}_{q'i'} Q^{m'\Sigma'}_{-qi} Q^{m'\Sigma'}_{f'q'} E_{\rm III} + Q^{m\Sigma}_{f-q} Q^{m\Sigma}_{-q'i'} Q^{m'\Sigma'}_{-qi} Q^{m'\Sigma'}_{f'-q'} E_{\rm IV}. \end{aligned} \tag{3.48}$$

The sums over the energy denominators, $E_{\rm I}$–$E_{\rm IV}$, for this graph are given in Appendix D.2. The diagram is thus split up into four parts as shown in Figure 3.5.

Once again, it is preferred to interpret the energy shift as a two-body operator $\hat{W}^{\rm II}$ inserted between a state $|\hat{X}\rangle$. Using Equation (3.33), it can easily be shown that this operator must have the form

$$W^{\mathcal{C}}_{12} = \frac{\alpha_{\rm S}^2}{R} \boldsymbol{F}_1 \cdot \boldsymbol{F}_2 \left(\boldsymbol{F}_1 \cdot \boldsymbol{F}_2 + \frac{3}{2}\right) \sum_{\Lambda} \nu^{\mathcal{C}}_{12}(\Lambda), \tag{3.49}$$

where Λ describes the angular momentum exchanged due to the effective interaction

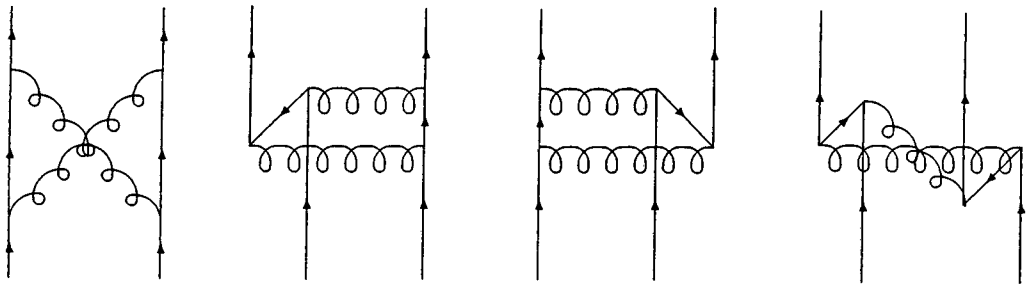

Figure 3.5: *These four diagrams represent the four terms in Equation (3.48) Again one notes the symmetry between terms II and III for identical interacting particles.*

of the two-gluon exchange. The terms $\nu_{12}^{\mathcal{C}}(\Lambda)$ can be written as

$$\begin{aligned}\nu_{12}^{\mathcal{C}}(\Lambda) &= -\sum_{\Sigma\Sigma'}\sum_{j_q j_{q'}}\sum_{J_1 J_2}\sum_{\lambda}\frac{g^{\Sigma\Sigma}\eta_\Sigma\, g^{\Sigma'\Sigma'}\eta_{\Sigma'}}{4\,\Omega_m^\Sigma R\,\Omega_{m'}^{\Sigma'}R} \\ &\quad\times G_{J_1J_2}(f,q,i')\,G_{J_2J_1}(f,q',i')\,\hat{\Lambda}^2\begin{Bmatrix} j_f & J_1 & j_q \\ J_2 & j_i & \Lambda\end{Bmatrix}\begin{Bmatrix} j_{f'} & J_1 & j_{q'} \\ J_2 & j_{i'} & \Lambda\end{Bmatrix} \\ &\quad\times(-1)^{1+\mu_{f'}-\mu_i}\begin{pmatrix} j_f & \Lambda & j_i \\ -\mu_f & \lambda & \mu_i\end{pmatrix}\begin{pmatrix} j_{f'} & \Lambda & j_{i'} \\ -\mu_{f'} & -\lambda & \mu_{i'}\end{pmatrix}\frac{\mathcal{C}}{R^3}, \end{aligned} \tag{3.50}$$

where $\mathcal{C}$ combines the radial integrals for the crossed diagram into one term

$$\begin{aligned}\mathcal{C} &= S_{fq}^{m\Sigma}\,S_{q'i'}^{m\Sigma}\,S_{qi}^{m'\Sigma'}\,S_{f'q'}^{m'\Sigma'}\,E_{\rm I} - S_{fq}^{m\Sigma}\,S_{-q'i'}^{m\Sigma}\,S_{qi}^{m'\Sigma'}\,S_{f'-q'}^{m'\Sigma'}\,E_{\rm II} \\ &- S_{f-q}^{m\Sigma}\,S_{q'i'}^{m\Sigma}\,S_{-qi}^{m'\Sigma'}\,S_{f'q'}^{m'\Sigma'}\,E_{\rm III} + S_{f-q}^{m\Sigma}\,S_{-q'i'}^{m\Sigma}\,S_{-qi}^{m'\Sigma'}\,S_{f'-q'}^{m'\Sigma'}\,E_{\rm IV}.\end{aligned} \tag{3.51}$$

If the matrix element is evaluated for external quarks in the ground state, then $j_n = \frac{1}{2}$ for $n = i, i', f, f'$, which implies only $\Lambda = 0, 1$ are allowed. One finds

$$\begin{aligned}\nu_{12}^{\mathcal{C}}(0) &= -\sum_{\Sigma\Sigma'}\sum_{J j_q j_{q'}}\frac{g^{\Sigma\Sigma}\eta_\Sigma\, g^{\Sigma'\Sigma'}\eta_{\Sigma'}}{4\,\Omega_m^\Sigma R\,\Omega_{m'}^{\Sigma'}R}\hat{j}_q^2\,\hat{j}_{q'}^2\,\hat{J}^2\,\delta_{J_1J_2}\begin{pmatrix}\frac{1}{2} & J & j_q \\ \frac{1}{2} & 0 & -\frac{1}{2}\end{pmatrix}^2 \\ &\quad\times\begin{pmatrix}\frac{1}{2} & J & j_{q'} \\ \frac{1}{2} & 0 & -\frac{1}{2}\end{pmatrix}^2\frac{\mathcal{C}}{R^3},\end{aligned} \tag{3.52}$$

$$\begin{aligned}\nu_{12}^{\mathcal{C}}(1) &= 8\,\boldsymbol{S}_1\cdot\boldsymbol{S}_2\sum_{\Sigma\Sigma'}\sum_{J j_q j_{q'}}\frac{g^{\Sigma\Sigma}\eta_\Sigma\, g^{\Sigma'\Sigma'}\eta_{\Sigma'}}{4\,\Omega_m^\Sigma R\,\Omega_{m'}^{\Sigma'}R}(-1)^{j_q+j_{q'}}\,\hat{j}_q^2\,\hat{j}_{q'}^2\,\hat{J}_1^2\,\hat{J}_2^2 \\ &\quad\times\begin{Bmatrix}\frac{1}{2} & J_1 & j_q \\ J_2 & \frac{1}{2} & 1\end{Bmatrix}\begin{Bmatrix}\frac{1}{2} & J_1 & j_{q'} \\ J_2 & \frac{1}{2} & 1\end{Bmatrix}\begin{pmatrix}\frac{1}{2} & J & j_q \\ \frac{1}{2} & 0 & -\frac{1}{2}\end{pmatrix}\end{aligned} \tag{3.53}$$

$$\times \begin{pmatrix} j_q & J & \frac{1}{2} \\ \frac{1}{2} & 0 & -\frac{1}{2} \end{pmatrix} \begin{pmatrix} \frac{1}{2} & J & j_{q'} \\ \frac{1}{2} & 0 & -\frac{1}{2} \end{pmatrix} \begin{pmatrix} j_{q'} & J & \frac{1}{2} \\ \frac{1}{2} & 0 & -\frac{1}{2} \end{pmatrix} \frac{C}{R^3}.$$

The sums and the radial integrals are again performed numerically. One has the same conditions from parity and angular momentum conservation as in the case for the straight two-gluon exchange.

The results for massless quarks and antiquarks are

	$\nu_{12}^{\mathcal{C}}(0)$
I	- 0.0728
II, III	0.1181
IV	- 0.0192

(3.54)

and

	$\nu_{12}^{\mathcal{C}}(1)$
I	- 0.0280 $\boldsymbol{S}_1 \cdot \boldsymbol{S}_2$
II, III	- 0.0563 $\boldsymbol{S}_1 \cdot \boldsymbol{S}_2$
IV	- 0.0485 $\boldsymbol{S}_1 \cdot \boldsymbol{S}_2$

(3.55)

3.3 Results

This chapter closes with a table of all the two-body operators (first and second order) for massless and massive quarks. The first order operator is given without the $\alpha_S \boldsymbol{F}_1 \cdot \boldsymbol{F}_2 / R$ part, the second order two-body operators for the straight and crossed diagrams are lacking a factor $\alpha_S^2 \, (\boldsymbol{F}_1 \cdot \boldsymbol{F}_2)^2 / R$ and $\alpha_S^2 \, \boldsymbol{F}_1 \cdot \boldsymbol{F}_2 \, (\boldsymbol{F}_1 \cdot \boldsymbol{F}_2 + \frac{3}{2}) / R$ respectively. The mass of the strange quark has been determined by adjusting it until the MIT mass formula, which is given in the following chapter, gives the experimentally determined mass for the Ω^-. It is found to be $m_s = 1.48$ fm^{-1}, corresponding to $m_s = 292.0$ MeV.

First Order			
m/fm^{-1}	$m_1 = m_2 = 0$	$m_1 = 1.48, m_2 = 0$	$m_1 = m_2 = 1.48$
V_{12}	$0.00980 - 0.70808 \, \boldsymbol{S}_1 \cdot \boldsymbol{S}_2$	$0.02292 - 0.56324 \, \boldsymbol{S}_1 \cdot \boldsymbol{S}_2$	$0.05389 - 0.45184 \, \boldsymbol{S}_1 \cdot \boldsymbol{S}_2$
Second Order, "Straight"			
m/fm^{-1}	$m_1 = m_2 = 0$	$m_1 = 1.48, m_2 = 0$	$m_1 = m_2 = 1.48$
W_{12}^S(I)	$-0.3637 + 0.5437 \, \boldsymbol{S}_1 \cdot \boldsymbol{S}_2$	$-0.3671 + 0.4533 \, \boldsymbol{S}_1 \cdot \boldsymbol{S}_2$	$-0.3926 + 0.4084 \, \boldsymbol{S}_1 \cdot \boldsymbol{S}_2$
W_{12}^S(II)	$0.0137 - 0.0016 \, \boldsymbol{S}_1 \cdot \boldsymbol{S}_2$	$0.0098 + 0.0021 \, \boldsymbol{S}_1 \cdot \boldsymbol{S}_2$	$0.0124 - 0.0081 \, \boldsymbol{S}_1 \cdot \boldsymbol{S}_2$
W_{12}^S(III)	$0.0137 - 0.0016 \, \boldsymbol{S}_1 \cdot \boldsymbol{S}_2$	$0.0171 - 0.0138 \, \boldsymbol{S}_1 \cdot \boldsymbol{S}_2$	$0.0124 - 0.0081 \, \boldsymbol{S}_1 \cdot \boldsymbol{S}_2$
W_{12}^S(IV)	$-0.0680 + 0.1874 \, \boldsymbol{S}_1 \cdot \boldsymbol{S}_2$	$-0.0561 + 0.1516 \, \boldsymbol{S}_1 \cdot \boldsymbol{S}_2$	$-0.0512 + 0.1377 \, \boldsymbol{S}_1 \cdot \boldsymbol{S}_2$
W_{12}^S	$-0.4043 + 0.7279 \, \boldsymbol{S}_1 \cdot \boldsymbol{S}_2$	$-0.3963 + 0.5932 \, \boldsymbol{S}_1 \cdot \boldsymbol{S}_2$	$-0.4190 + 0.5299 \, \boldsymbol{S}_1 \cdot \boldsymbol{S}_2$
Second Order, "Crossed"			
m/fm^{-1}	$m_1 = m_2 = 0$	$m_1 = 1.48, m_2 = 0$	$m_1 = m_2 = 1.48$
W_{12}^C(I)	$-0.0728 - 0.0280 \, \boldsymbol{S}_1 \cdot \boldsymbol{S}_2$	$-0.0696 + 0.0030 \, \boldsymbol{S}_1 \cdot \boldsymbol{S}_2$	$-0.0723 + 0.0284 \, \boldsymbol{S}_1 \cdot \boldsymbol{S}_2$
W_{12}^C(II)	$0.1181 - 0.0563 \, \boldsymbol{S}_1 \cdot \boldsymbol{S}_2$	$0.1083 - 0.0191 \, \boldsymbol{S}_1 \cdot \boldsymbol{S}_2$	$0.0806 + 0.0240 \, \boldsymbol{S}_1 \cdot \boldsymbol{S}_2$
W_{12}^C(III)	$0.1181 - 0.0563 \, \boldsymbol{S}_1 \cdot \boldsymbol{S}_2$	$0.0861 - 0.0005 \, \boldsymbol{S}_1 \cdot \boldsymbol{S}_2$	$0.0806 + 0.0240 \, \boldsymbol{S}_1 \cdot \boldsymbol{S}_2$
W_{12}^C(IV)	$-0.0192 - 0.0485 \, \boldsymbol{S}_1 \cdot \boldsymbol{S}_2$	$-0.0220 - 0.0555 \, \boldsymbol{S}_1 \cdot \boldsymbol{S}_2$	$-0.0252 - 0.0648 \, \boldsymbol{S}_1 \cdot \boldsymbol{S}_2$
W_{12}^C	$0.1442 - 0.1891 \, \boldsymbol{S}_1 \cdot \boldsymbol{S}_2$	$0.1028 - 0.0721 \, \boldsymbol{S}_1 \cdot \boldsymbol{S}_2$	$0.0637 + 0.0116 \, \boldsymbol{S}_1 \cdot \boldsymbol{S}_2$

Table 3.1: *The two-body operators for the one- and two-gluon exchange diagrams.*

It is noted that, the results for the two-body operators for the massless quarks are in good agreement with the results obtained by Stoddart [36], if one only considers the diagrams labeled I. For two quarks coupled to $J = 0$ he obtained -0.764

and -0.050 for the straight and crossed diagrams respectively, while the results found here are -0.771 and -0.052. Two quarks coupled to $J = 1$ yielded -0.226 and -0.079 in Stoddart's work, while they are -0.228 and -0.080 in this thesis. In [37], the two-body operators are listed and they also agree very well with the corresponding ones from Table 3.1. However, the argument, that the contributions from the other diagrams are negligible is not valid for the crossed diagrams, where they amount to the major contributions to the two-body operators.

Chapter 4

The Hadron Spectrum

In the previous chapter, it has been shown, that the energy shifts due to the one- and two-gluon exchange Feynman diagrams can be expressed in the form of a two-body operator. The knowledge of these two-body operators allows one to calculate the masses of mesons and baryons with up to second order perturbative corrections. However, first one needs to find a way to evaluate the two-body operators for two- and three-body systems.

4.1 Evaluation of the Two-Body Operators

The energy shift to be calculated, is the expectation value of the following operator

$$\Delta E = \frac{1}{2}\sum_{i\neq j} V_{ij}, \tag{4.1}$$

where V_{ij} is one of the two-body operators found in the previous chapter, and it is of the form

$$(a + b\,\boldsymbol{F}_i \cdot \boldsymbol{F}_j)(\mu(0) + \mu(1)\,\boldsymbol{S}_i \cdot \boldsymbol{S}_j). \tag{4.2}$$

The coefficients $\mu(0)$ and $\mu(1)$ depend on the mass of the interacting particles. They are different for two massless (up- or down-) quarks, a massless and a massive (strange) quark, and two massive quarks, as can be seen from Table 3.1.

For mesons, Equation (4.1) is easily evaluated, since only two particles, a quark and an antiquark are involved. These are in a colour singlet state, i.e.

$$\boldsymbol{F}_1 + \boldsymbol{F}_2 = 0, \tag{4.3}$$

so

$$\boldsymbol{F}_1 \cdot \boldsymbol{F}_2 = -\boldsymbol{F}^2 = -\frac{4}{3}. \tag{4.4}$$

The operator $\boldsymbol{S}_1 \cdot \boldsymbol{S}_2$ is just as easily found by using

$$\boldsymbol{J} = \boldsymbol{S}_1 + \boldsymbol{S}_2, \tag{4.5}$$

therefore

$$\boldsymbol{S}_1 \cdot \boldsymbol{S}_2 = \frac{1}{2}\left(J(J+1) - \frac{3}{2}\right), \tag{4.6}$$

which yields

$$\boldsymbol{S}_1 \cdot \boldsymbol{S}_2 = \begin{cases} \frac{1}{4} & \text{for } J = 1, \\ -\frac{3}{4} & \text{for } J = 0. \end{cases} \tag{4.7}$$

Finally, the energy shift for mesons can be written as

$$\Delta E = \left(a - \frac{4}{3}b\right)\left(\mu(0) + \frac{1}{2}\left(J(J+1) - \frac{3}{2}\right)\mu(1)\right), \tag{4.8}$$

where the coefficients are determined by the strange quark content of the mesons. and J is the spin of the mesons.

For baryons, one can also easily evaluate the colour factor $\boldsymbol{F}_i \cdot \boldsymbol{F}_j$, by exploiting the fact that they are also in a colour singlet state, ie.

$$\boldsymbol{F}_1 + \boldsymbol{F}_2 + \boldsymbol{F}_3 = 0. \tag{4.9}$$

Multiplying the above by $\boldsymbol{F}_1$, one finds

$$\boldsymbol{F}_1^2 + \boldsymbol{F}_1 \cdot \boldsymbol{F}_2 + \boldsymbol{F}_1 \cdot \boldsymbol{F}_3 = 0, \tag{4.10}$$

and two similar equations are obtained by multiplying by $\boldsymbol{F}_2$ and $\boldsymbol{F}_3$. These three equations yield

$$\boldsymbol{F}_1 \cdot \boldsymbol{F}_2 = \boldsymbol{F}_1 \cdot \boldsymbol{F}_3 = \boldsymbol{F}_2 \cdot \boldsymbol{F}_3 = -\frac{2}{3}. \tag{4.11}$$

The colour factor can therefore be extracted from the sum in Equation (4.1).

The calculation of the remaining sum

$$\frac{1}{2}\sum_{i \neq j} \mu(1)\, \boldsymbol{S}_i \cdot \boldsymbol{S}_j \tag{4.12}$$

is a little more complicated, since one needs to know the valence quark content of the particular baryon. If the baryon contains either massless or massive quarks, one can easily see that

$$\frac{1}{2}\sum_{i\neq j} \boldsymbol{S}_i \cdot \boldsymbol{S}_j = \frac{1}{2}\left(J(J+1) - \frac{9}{4}\right), \tag{4.13}$$

therefore

$$\frac{1}{2}\sum_{i\neq j} \boldsymbol{S}_i \cdot \boldsymbol{S}_j = \begin{cases} \frac{3}{4} & \text{for } J = \frac{3}{2}, \\ -\frac{3}{4} & \text{for } J = \frac{1}{2}. \end{cases} \tag{4.14}$$

Knowing the wavefunction of a baryon also allows one to calculate the sum for quarks with different masses by using

$$2\,\boldsymbol{S}_u \cdot \boldsymbol{S}_s = \frac{1}{2}\sum_{i\neq j} \boldsymbol{S}_i \cdot \boldsymbol{S}_j - \boldsymbol{S}_u \boldsymbol{S}_u. \tag{4.15}$$

For example, for a $\Sigma^+(1193)$ hyperon (uus) from the $SU(3)$ octet, the two up quarks are in a triplet spin state, thus $2\,\boldsymbol{S}_u \cdot \boldsymbol{S}_s = -1$. while for a $\Lambda^0(1116)$ (uds), the up and down quarks are in a singlet spin state, therefore $2\,\boldsymbol{S}_u \cdot \boldsymbol{S}_s = 0$. Consequently, one can expect a splitting of the Λ and the Σ, which is not obvious from the quark content.

Table 4.1 lists the results of $\frac{1}{2}\sum_{i\neq j}(\mu(0) + \mu(1)\,\boldsymbol{S}_i \cdot \boldsymbol{S}_j)$ sandwiched between various baryons from the $SU(3)$ decuplet and octet. Only the most positively charged member of each multiplet is listed.

4.2 The MIT Mass Formula

In the MIT bag model, the empty bag has an energy proportional to its volume. This is the volume energy due to an external pressure B,

$$E_B = \frac{4}{3}\pi R^3 B. \tag{4.16}$$

If the cavity contains quarks or antiquarks, their energy has to be added to the volume energy,

$$E_q = \sum_q \frac{\omega_q}{R}. \tag{4.17}$$

Furthermore, one has to include an additional term E_0, which allows one to adjust the mass and radius difference between mesons and baryons,

$$E_0 = -\frac{Z_0}{R}, \quad Z_0 = \text{const.} \tag{4.18}$$

Decuplet Baryons	
Δ^{++}	Ω^-
$3(\mu(0)+\mu(1)/4)$	$3(\mu''(0)+\mu''(1)/4)$
Σ^*	Ξ^*
$\mu(0)+\mu(1)+2(\mu'(0)+\mu'(1)/4)$	$2(\mu'(0)+\mu'(1)/4)+\mu''(0)+\mu''(1)/4$
Octet Baryons	
p	Σ^+
$3(\mu(0)-\mu(1)/4)$	$\mu(0)+\mu(1)/4+2\mu'(0)-\mu'(1)$
Λ^0	Ξ^0
$\mu(0)-3\mu(1)/4+2\mu'(0)$	$2\mu'(0)-\mu'(1)+\mu''(0)+\mu''(1)$

Table 4.1: *Evaluation of the operator* $\frac{1}{2}\sum_{i\neq j}(\mu(0)+\mu(1)\,S_i\cdot S_j)$ *for various baryons from the decuplet and octet. The different coefficients* μ, μ' *and* μ'' *stand for interactions involving two massless particles, a massive and a massless particle and two massive particles respectively.*

This term, the so-called zero-point energy, may be interpreted as the *Casimir effect* [49]. The first and second order perturbative corrections are the final terms needed to obtain the total energy of a hadron. They are functions of α_S and $1/R$,

$$E_p = \frac{1}{2}\sum_{i\neq j}(V_{ij}+W_{ij}). \tag{4.19}$$

The total energy of a hadron is thus

$$E(R) = E_B + E_0 + E_q + E_p. \tag{4.20}$$

The mass of the hadron is now found by minimizing the energy with respect to the bag radius. The radial dependence is of the form

$$E(R) = \frac{A}{R} + \frac{4}{3}\pi R^3 B, \tag{4.21}$$

where A is dependent on α_S and Z_0,

$$A = f(\alpha_S, \alpha_S^2) - Z_0. \tag{4.22}$$

It is easily shown that

$$R^4 = \frac{A}{4\pi B} \tag{4.23}$$

and therefore

$$M = \frac{4}{3}(4\pi)^{\frac{1}{4}} B^{\frac{1}{4}} A^{\frac{3}{4}}. \tag{4.24}$$

Clearly,

$$\left(\frac{M_2}{M_1}\right)^{\frac{4}{3}} = \frac{A_2}{A_1}. \tag{4.25}$$

Thus given three masses, i.e. two ratios, one can solve for α_S, Z_0 and B.

4.3 The Hadron Spectrum

The masses for various strange and non-strange hadrons can be calculated from Equation (4.24). The up and down quarks are known to have a very small mass, and the model is not sensitive to these small values. They are thus set to zero. The parameters α_S, Z_0 and B are determined by inserting the masses of three non-strange hadrons, namely proton, Δ and ω into Equation (4.25). Using these three parameters in Equation (4.24), the mass of the strange quark is varied until the experimentally determined mass of the Ω^- is obtained. This process is quite tedious, since the calculations for the second order interactions are very time consuming. The parameters are found to be:

$$\alpha_S = 1.033, \tag{4.26}$$

$$Z_0 = 1.333, \tag{4.27}$$

$$B^{\frac{1}{4}} = 154.9 \text{ MeV}, \tag{4.28}$$

$$m_s = 1.48 \text{ fm}^{-1} = 292.0 \text{ MeV}. \tag{4.29}$$

Table 4.2 and Figure 4.1 show the results. The η and η' have not been included because with the interactions considered in this thesis, the η' and the pion are degenerate. The degeneracy can be lifted by including the two-gluon annihilation graphs, since these interactions only affect the isoscalars, namely the η and η'.

One notes an extremely good agreement between the predicted masses and the experimental values for the decuplet baryons. This is partly due to the fact that two of the four decuplet baryon masses are used to fix the free parameters. The

masses of the octet baryons are also predicted very well. The splitting of the Λ and the Σ is much better than in the original fit [20] which included only the first order interactions.

The calculated masses for the vector mesons are in agreement with the experimental values to about 10%. This is not quite satisfactory, considering the excellent results for the baryon masses, and may be a result of the fitting of the mass of the strange quark to the Ω^-. The validity of this argument may be questioned in view of the nearly perfect agreement between theory and experiment on the mass of the kaons. The pions remain a problem, although in the bag model including all the two-gluon exchange diagrams, the coefficient A in Equation (4.24) is positive and an estimate of the π-mass was possible. The pion mass is very much dependent on the model parameters and the interactions included in the calculations. For instance, Stoddart [36] included only the two-gluon exchange diagrams labeled here $W^S(\mathrm{I})$ and $W^C(\mathrm{I})$, and obtained a negative coefficient A, which obviously does not allow for the calculation of a mass for the pion, so it was set to zero. The value found here is smaller than the experimental value by about 40%.

Particle	M_{exp} (MeV)	M_{bag} (MeV)	R (fm)
Δ	<u>1232</u>	1232	0.994
Σ^*	1385	1385	1.033
Ξ^*	1533	1532	1.068
Ω^-	<u>1672</u>	1672	1.100
p	<u>938</u>	938	0.907
Λ	1116	1129	0.965
Σ	1189	1176	0.978
Ξ	1321	1330	1.019
ρ	770	782	0.854
ω	<u>782</u>	782	0.854
K^*	892	950	0.911
ϕ	1019	1102	0.957
π	140	86	0.409
K	494	493	0.732

Table 4.2: *Experimental and predicted masses of various hadrons. The underlined masses have been used to fix the parameters of the model.*

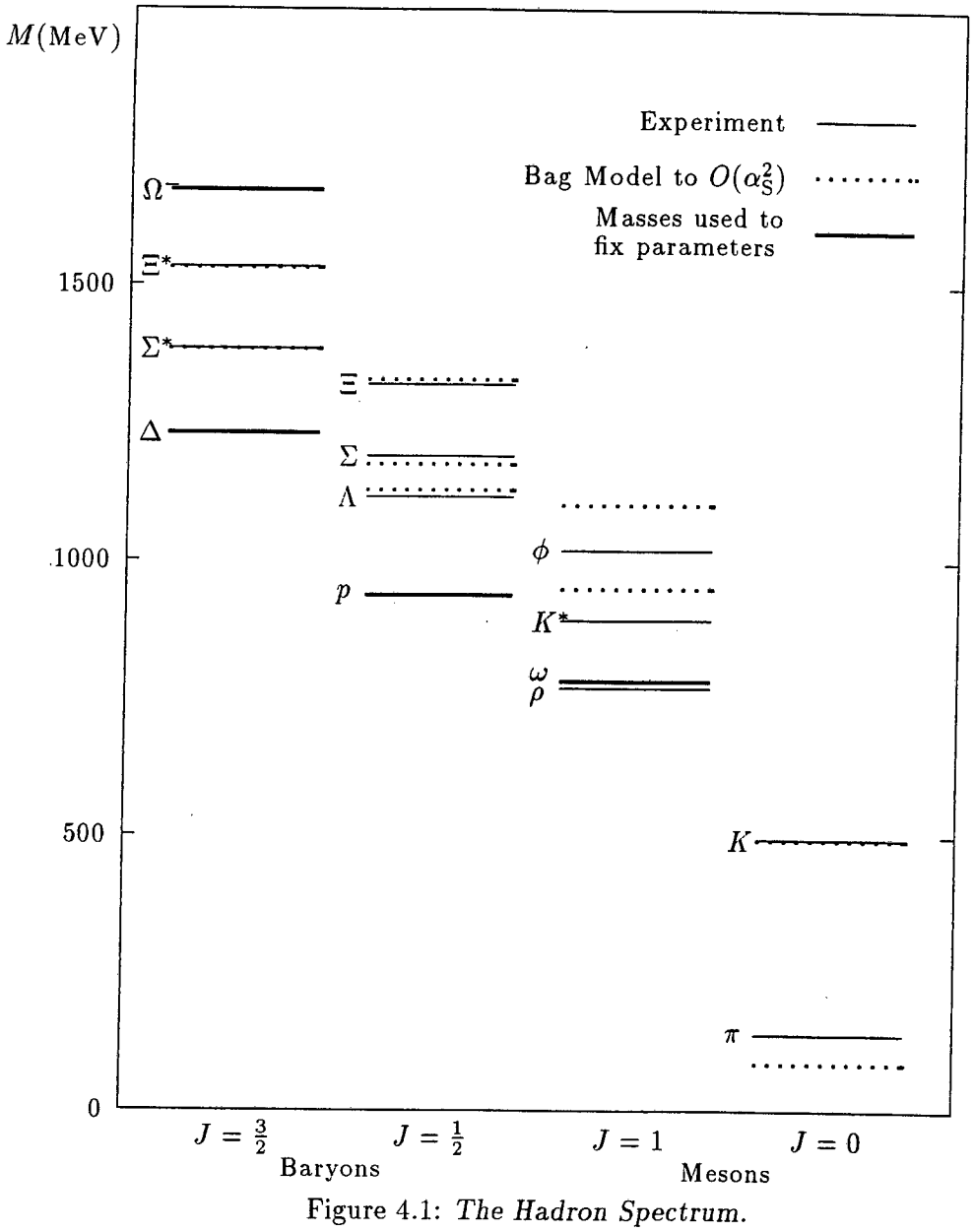

Figure 4.1: *The Hadron Spectrum.*

Chapter 5

Conclusion

The formalism of cavity quantum chromodynamics as developed by Buser *et al.* is a powerful tool to investigate properties of hadrons. Here, the second order perturbative corrections due to the two-gluon exchange Feynman diagrams have been calculated in full for the first time. The results obtained agree well, within computational accuracy restrictions, with the partial calculations done by A. Stoddart *et al.*, even though the methods used are quite different.

As an application of the obtained two-body operators for the energy shift due to the second order interactions, the mass spectrum for baryons and mesons has been calculated. There are four parameters in the model, the strong coupling constant α_S, the zero-point energy Z_0, the bag pressure B and the mass of the strange quark m_s. The parameters are fixed with the help of four of the total of fourteen masses available for the hadrons containing up, down and strange quarks and antiquarks. The agreement between experimental and predicted values is very good except for the pions.

The inclusion of second order corrections lowers the value for α_S to a more reasonable value close to one from a value larger than two in the original MIT bag model fit. A smaller value is desirable if one relies on perturbative calculations. On the other hand, the total contributions from the second order diagrams are usually larger than the first order corrections. This put some doubt on the validity of perturbation theory. One could possibly work out third order corrections to see if this trend continues. However, the practicality of this proposal is doubtful, since the

second order calculations already involve extremely lengthy numerical calculations (some 100,000 evaluations of radial integrals for each of the coefficients in Table 3.1). Another order would involve sums over three more cavity modes, ie. over six further quantum numbers.

No attempt to fit the masses of the isoscalar mesons η and η' have been made in this thesis. It would be interesting to also complete the calculations of the two-gluon annihilation graphs started by Stoddart, since these are responsible for the splitting of the degeneracy of the η' and the π.

An expansion of this work should include the self-energy corrections for the quarks and gluons in the cavity which have been ignored here. The vertex correction diagrams should also be included, if one wants to obtain a complete set of second order corrections.

Another interesting field for cavity quantum chromodynamics has opened up with the recent discovery of exotic states [50]. All the calculations done here can be easily expanded to those exotic states.

Acknowledgements

Many thanks to my supervisor, Prof. R. D. Viollier, for his support and guidance, as well as for his patience and encouragement. Dr. R. J. Lindebaum deserves special thanks for his time and effort, always ready to help with any problem that I came across. I am grateful to Desireé Thomas for her help with the preparation of this thesis.

Appendix A

The Cavity Modes

The derivations of the quark and gluon cavity modes are outlined in this appendix following the approach of Buser *et al.* [21].

A.1 The Quark Cavity Modes

The cavity modes of quarks in a spherical symmetric and static cavity are solutions of the time independent Dirac equation constrained by the boundary conditions of the MIT bag model.

$$(-i\boldsymbol{\gamma}\cdot\boldsymbol{\nabla}+m_f)u_n(\mathbf{r})=\varepsilon_n\gamma^0u_n(\mathbf{r}), \tag{A.1}$$

where ε_n is the energy and m_f the mass of the quark. The solutions are given by Dirac spinors

$$u_n(\mathbf{r})=\begin{pmatrix} g_n(r)\chi^\mu_\kappa(\hat{\mathbf{r}}) \\ if_n(r)\chi^\mu_{-\kappa}(\hat{\mathbf{r}})\end{pmatrix}, \tag{A.2}$$

where $\chi^\mu_\kappa(\hat{\mathbf{r}})$ is the usual two-component spherical spinor. The index n denotes the flavor, radial, Dirac and magnetic quantum numbers of the spinor, i.e.

$$n=\{f,\nu,\kappa,\mu\}. \tag{A.3}$$

The radial functions $g_n(r)$ and $f_n(r)$ are given in terms of the spherical Bessel functions j_l by

$$g_n(r) = \frac{\mathcal{N}_n}{R^{3/2}}j_l(p_nr) \tag{A.4}$$

$$f_n(r) = \frac{\mathcal{N}_np_n\,\mathrm{sgn}\,\kappa}{R^{3/2}(\varepsilon_n+m_f)}j_{\tilde{l}}(p_nr), \tag{A.5}$$

where R is the radius of the cavity. The total (j) and orbital (l,$\bar{l}$) angular momenta are defined as functions of the Dirac quantum number κ:

$$j(\kappa) = |\kappa| - \frac{1}{2} \tag{A.6}$$

$$l(\kappa) = j(\kappa) + \frac{1}{2}\text{sgn } \kappa \tag{A.7}$$

$$\bar{l}(\kappa) = j(\kappa) - \frac{1}{2}\text{sgn } \kappa. \tag{A.8}$$

One should note that the positive and negative energy solutions of the Dirac equation are denoted by $\nu > 0$ and $\nu < 0$ respectively. The quark momenta, introduced in the radial functions g_n and f_n, are determined by the boundary conditions of the MIT bag model

$$(i\gamma\cdot\hat{\mathbf{r}} + 1)u_n(\mathbf{r})|_{r=R} = 0 \tag{A.9}$$

which leads to the eigenvalue equation

$$j_l(x_n) + \frac{x_n \text{sgn } \kappa}{\omega_n + \zeta_f} j_{\bar{l}}(x_n) = 0. \tag{A.10}$$

Here the dimensionless energy, momentum, and mass parameters have been introduced:

$$\omega_n = \varepsilon_n R = \text{sgn } \nu \sqrt{x_n^2 + \zeta_f^2}, \tag{A.11}$$

$$x_n = p_n R, \tag{A.12}$$

$$\zeta_f = m_f R. \tag{A.13}$$

The normalization constant $\mathcal{N}_n$ is given by

$$\mathcal{N}_n = (2\omega_n(\omega_n + \kappa) + \zeta_f)^{-\frac{1}{2}} \left| \frac{x_n}{j_l(x_n)} \right| \tag{A.14}$$

The solutions (A.2) of the Dirac equation (A.1) satisfying the boundary condition (A.9) are a complete and orthonormal set of Dirac spinors in the cavity, i.e. they satisfy the relations

$$\int u_n^+(\mathbf{r}) u_{n'}(\mathbf{r}) d^3r = \delta_{nn'}, \tag{A.15}$$

$$\sum_{\nu\kappa\mu} u_{n\alpha}^*(\mathbf{r}) u_{n\beta}(\mathbf{r}') = \delta_{\alpha\beta}\delta^3(\mathbf{r} - \mathbf{r}'), \tag{A.16}$$

where $u_{n\alpha}(\mathbf{r})$ denotes the component α of the Dirac spinor $u_n(\mathbf{r})$.

A.2 The Gluon Cavity Modes

In the Feynman gauge ($\lambda = 1$) the gluon cavity modes are solutions of the time independent d'Alambert equation

$$(\Delta + \Omega_{m\Sigma}^2) a_{m\Sigma}(\mathbf{r}) = 0, \qquad \Sigma = \mathcal{S}, \mathcal{L}, \mathcal{M}, \mathcal{E} \tag{A.17}$$

where Σ labels the polarization of the solutions of these equations. They describe the scalar, longitudinal, transverse magnetic, and transverse electric polarization respectively. The index $m = \{N, J, M\}$ denotes the radial, total angular momentum and magnetic quantum numbers of the eigenmodes respectively. The solutions can be given in terms of the spherical Bessel functions and the vector spherical harmonics:

$$a^0_{m\mathcal{S}}(\mathbf{r}) = \frac{\mathcal{N}_{m\mathcal{S}}}{R^{3/2}} i j_J(\Omega^{\mathcal{S}}_m r) Y_{JM}(\hat{\mathbf{r}}) \tag{A.18}$$

$$\mathbf{a}_{m\mathcal{L}}(\mathbf{r}) = \frac{\mathcal{N}_{m\mathcal{L}}}{\sqrt{R^3(2J+1)}} \left[\sqrt{J} j_{J-1}(\Omega^{\mathcal{L}}_m r)\mathbf{Y}^{J-1}_{JM}(\hat{\mathbf{r}}) + \sqrt{J+1} j_{J+1}(\Omega^{\mathcal{L}}_m r)\mathbf{Y}^{J+1}_{JM}(\hat{\mathbf{r}})\right] \tag{A.19}$$

$$\mathbf{a}_{m\mathcal{M}}(\mathbf{r}) = \frac{\mathcal{N}_{m\mathcal{M}}}{R^{3/2}} j_J(\Omega^{\mathcal{M}}_m r)\mathbf{Y}^{J}_{JM}(\hat{\mathbf{r}}) \tag{A.20}$$

$$\mathbf{a}_{m\mathcal{E}}(\mathbf{r}) = \frac{\mathcal{N}_{m\mathcal{E}}}{\sqrt{R^3(2J+1)}} \left[\sqrt{J+1} j_{J-1}(\Omega^{\mathcal{E}}_m r)\mathbf{Y}^{J-1}_{JM}(\hat{\mathbf{r}}) - \sqrt{J} j_{J+1}(\Omega^{\mathcal{E}}_m r)\mathbf{Y}^{J+1}_{JM}(\hat{\mathbf{r}})\right]. \tag{A.21}$$

Here the total angular momentum $J \geq 0$ for $\Sigma = \mathcal{S}, \mathcal{L}$ and $J \geq 1$ for $\Sigma = \mathcal{M}, \mathcal{E}$. The gluon energies are determined by the MIT boundary conditions

$$\hat{\mathbf{r}}\cdot\nabla a^{\mathcal{S}}_m(\mathbf{r})|_{r=R} = 0 \tag{A.22}$$

$$\hat{\mathbf{r}}\cdot\mathbf{a}^{\Sigma}_m(\mathbf{r})|_{r=R} = 0 \tag{A.23}$$

$$\hat{\mathbf{r}} \times (\nabla \times \mathbf{a}^{\Sigma}_m(\mathbf{r}))|_{r=R} = 0; \qquad \Sigma = \mathcal{L}, \mathcal{M}, \mathcal{E} \tag{A.24}$$

which can be reduced to the following eigenvalue equations:

$$J j_J(\Omega^{\Sigma}_m R) - \Omega^{\Sigma}_m R j_{J+1}(\Omega^{\Sigma}_m R) = 0, \qquad \Sigma = \mathcal{S}, \mathcal{L} \tag{A.25}$$

$$(J+1) j_J(\Omega^{\mathcal{M}}_m R) - \Omega^{\mathcal{M}}_m R j_{J+1}(\Omega^{\mathcal{M}}_m R) = 0, \tag{A.26}$$

$$j_J(\Omega^{\mathcal{E}}_m R) = 0. \tag{A.27}$$

The scalar and longitudinal modes therefore have the same energy spectrum, with the exception of the zero energy scalar mode, which has no corresponding longitu-

dinal mode. The normalization constants are given by

$$\mathcal{N}_{m\Sigma} = \sqrt{\frac{2}{(\Omega_m^\Sigma R)^2 - J(J+1)}} \left| \frac{\Omega_m^\Sigma R}{j_J(\Omega_m^\Sigma R)} \right|, \qquad \Sigma = \mathcal{S}, \mathcal{L}, \mathcal{M} \quad \text{(A.28)}$$

$$\mathcal{N}_{m\mathcal{E}} = \frac{\sqrt{2}}{|j_{J+1}(\Omega_m^\mathcal{E} R)|}. \quad \text{(A.29)}$$

The zero energy scalar mode has the quantum numbers $m_0 = \{0,0,0\}$ and is just a constant

$$a_{m_0\mathcal{S}} = i\sqrt{\frac{3}{4\pi}}. \quad \text{(A.30)}$$

The set of gluon modes (A.18) – (A.21) is complete and orthonormal in the cavity, i.e.

$$\sum_{m\Sigma} g^{\Sigma\Sigma} a^\mu_{m\Sigma}(\mathbf{r}) a^{\nu *}{}_{m\Sigma}(\mathbf{r}') = g^{\mu\nu}\delta^{(3)}(\mathbf{r},\mathbf{r}') \quad \text{(A.31)}$$

$$\int d^3r\, g_{\mu\nu} a^\mu_{m\Sigma}(\mathbf{r}) a^{\nu *}{}_{m'\Sigma'}(\mathbf{r}) = g^{\Sigma\Sigma'}\delta_{mm'}, \quad \text{(A.32)}$$

where $g^{\Sigma\Sigma'}$ is the diagonal metric tensor in polarization space which is defined as:

$$g^{\mathcal{S}\mathcal{S}} = -g^{\mathcal{L}\mathcal{L}} = -g^{\mathcal{M}\mathcal{M}} = -g^{\mathcal{E}\mathcal{E}} = 1, \qquad g^{\Sigma\Sigma'} = 0 \text{ for } \Sigma \neq \Sigma'. \quad \text{(A.33)}$$

Under complex conjugation the gluon cavity modes transform in the following manner:

$$a^{\mu *}_{m\Sigma} = \eta_\Sigma (-1)^M a^\mu_{m^*\Sigma}(\mathbf{r}), \quad \text{(A.34)}$$

where the set of quantum numbers m^* is defined as

$$m^* = \{N, J, -M\} \quad \text{(A.35)}$$

and the phase η_Σ is given by

$$\eta_\Sigma = \begin{cases} +1 & \text{for } \Sigma = \mathcal{L}, \mathcal{E}, \\ -1 & \text{for } \Sigma = \mathcal{S}, \mathcal{M}. \end{cases} \quad \text{(A.36)}$$

One often needs the product $g^{\Sigma\Sigma}\eta_\Sigma$, so it is briefly noted that

$$g^{\Sigma\Sigma}\eta_\Sigma = \begin{cases} -1 & \text{for } \Sigma \neq \mathcal{M}, \\ +1 & \text{for } \Sigma = \mathcal{M}. \end{cases} \quad \text{(A.37)}$$

Appendix B

The Quark-Gluon Vertex Integrals

In the context of the Gell-Mann and Low theorem, the interaction between a quark and a gluon always leads to an integral over two quark and one gluon fields

$$Q^{m\Sigma}_{nn'} = i \int d^3r \bar{u}_n(\vec{r}) \gamma_\mu u_{n'}(\vec{r}) a^\mu_{m\Sigma}(\vec{r}) \tag{B.1}$$

and an integral in which the gluon field is replaced by its complex conjugate

$$\tilde{Q}^{m\Sigma}_{nn'} = i \int d^3r \bar{u}_n(\vec{r}) \gamma_\mu u_{n'}(\vec{r}) a^{\mu *}_{m\Sigma}(\vec{r}). \tag{B.2}$$

Both integrals (B.1) and (B.2) are related due to the relation (A.34)

$$\tilde{Q}^{m\Sigma}_{nn'} = (-1)^M \eta^\Sigma Q^{m^*\Sigma}_{nn'} = -Q^{m\Sigma}_{n'n}. \tag{B.3}$$

The vertex integrals involving the scalar and longitudinal modes are related by current conservation,

$$Q^{m\mathcal{L}}_{nn'} = \frac{\varepsilon_{n'} - \varepsilon_n}{\Omega^{\mathcal{S}}_m} Q^{m\mathcal{S}}_{nn'} \tag{B.4}$$

which is valid for all but the zero energy scalar mode.

Following the approach by Viollier *et al.* [45], the vertex integrals can be separated into radial and angular parts as

$$\begin{aligned} Q^{m\Sigma}_{nn'} &= R^{-3/2} R^{m\Sigma}_{nn'} \int d\Omega \chi^{\mu\dagger}_\kappa(\hat{r}) Y_{JM}(\hat{r}) \chi^{\mu'}_{\kappa'}(\hat{r}) \qquad \Sigma = \mathcal{S}, \mathcal{L}, \mathcal{E} \\ Q^{m\mathcal{M}}_{nn'} &= R^{-3/2} R^{m\mathcal{M}}_{nn'} \int d\Omega \chi^{\mu\dagger}_\kappa(\hat{r}) Y_{JM}(\hat{r}) \chi^{\mu'}_{-\kappa'}(\hat{r}). \end{aligned} \tag{B.5}$$

The integrals over the angular variables can be performed by expanding the spinor spherical harmonics in a Clebsch-Gordan series. One obtains

$$\begin{aligned}\int d\Omega \chi^{\mu\dagger}_{\kappa}(\hat{r}) Y_{JM}(\hat{r}) \chi^{\mu'}_{\pm\kappa'}(\hat{r}) &= \frac{(-1)^{\mu+\frac{1}{2}}}{\sqrt{4\pi}} \frac{(1\pm(-1)^{l+J+l'})}{2} \hat{j}\hat{J}\hat{j}' \\ &\begin{pmatrix} j & J & j' \\ \frac{1}{2} & 0 & -\frac{1}{2} \end{pmatrix} \begin{pmatrix} j & J & j' \\ -\mu & M & \mu \end{pmatrix}, \end{aligned} \tag{B.6}$$

where the abbreviation $\hat{j} = \sqrt{2j+1}$ is used. The notation for the 3j-symbols is that used by Edmonds [51, p. 46]. The radial integrals are

$$R^{m\mathcal{S}}_{nn'} = -\mathcal{N}_{m\mathcal{S}} \int_0^R dr\, r^2 j_J(\Omega^{\mathcal{S}}_m r) S_{nn'}(r) \tag{B.7}$$

$$R^{m\mathcal{L}}_{nn'} = \frac{\varepsilon_{n'} - \varepsilon_n}{\Omega^{\mathcal{S}}_m} R^{m\mathcal{S}}_{nn'} \tag{B.8}$$

$$R^{m\mathcal{M}}_{nn'} = -\frac{\mathcal{N}_{m\mathcal{M}}(\kappa+\kappa')}{\sqrt{J(J+1)}} \int_0^R dr\, r^2 j_J(\Omega^{\mathcal{M}}_m r) T_{nn'}(r) \tag{B.9}$$

$$\begin{aligned} R^{m\mathcal{E}}_{nn'} = -\frac{\mathcal{N}_{m\mathcal{E}}}{\Omega^{\mathcal{E}}_m \sqrt{J(J+1)}} \int_0^R dr\, r \Big(& J(J+1) j_J(\Omega^{\mathcal{E}}_m r) U_{nn'}(r) \\ & + (\kappa - \kappa')[J j_J(\Omega^{\mathcal{E}}_m r) - \Omega^{\mathcal{E}}_m r j_{J-1}(\Omega^{\mathcal{E}}_m r)] T_{nn'}(r) \Big), \end{aligned} \tag{B.10}$$

where the functions $S_{nn'}$, $T_{nn'}$ and $U_{nn'}$ are defined in terms of the radial parts of the quark wave function as

$$S_{nn'} = g_n g_{n'} + f_n f_{n'} \tag{B.11}$$

$$T_{nn'} = g_n f_{n'} + f_n g_{n'} \tag{B.12}$$

$$U_{nn'} = g_n f_{n'} - f_n g_{n'}, \tag{B.13}$$

where the functions g_n and f_n are defined in Equations (A.4) and (A.5) respectively.

Appendix C

Numerical Methods

Unfortunately, one does not get very far in cavity QCD without performing numerical calculations. This appendix outlines the numerical methods used to calculate energy shifts up to second order in α_S as well as some of the necessary relations for the coupling of angular momenta.

C.1 Spherical Bessel Functions

The basis of many of the numerical calculations is the evaluation of spherical Bessel functions, which need to be evaluated to find the eigenenergies of the quark and gluon states. They are also the main ingredients in the radial parts of the quark-gluon vertex integrals. Three different methods are used to maximize the speed of the convergence. The choice of the method used is dependent on the relation between x and l. The different methods are:

- Forward recursion in the region $x \geq l$:

$$j_{l+1}(x) = \frac{2l}{x} j_l(x) - j_{l-1}(x), \quad j_0(x) = \frac{\sin x}{x}, \quad j_1(x) = \frac{\sin x}{x^2} - \frac{\cos x}{x}. \quad \text{(C.1)}$$

- Series expansion in the region $x < l/4 + 15$, except where forward recursion works:

$$j_l(x) = \left(\frac{x}{2}\right)^l \sum_{k=0}^{\infty} \frac{(-x/2)^{2k}}{k!\Gamma(l+k+1)} \quad \text{(C.2)}$$

- Reverse recursion as in [52] in the remaining region.

The speed of the calculation of the spherical Bessel functions is essential because of the central role of the spherical Bessel functions in all the calculations.

C.2 Energies of the Cavity Modes

The first calculation to be performed is the evaluation of the various cavity modes for quarks and gluons. The necessary equations have been derived in Appendix A and are given in Equations (A.10) and (A.25)–(A.27) respectively. These are relatively easily solved using the secant method [53]. This method assumes approximate linearity of the function near the root, which is the case for Bessel functions. The roots are then saved into a file which is reused by all other programs.

C.3 Quark-Gluon Vertex Integrals

The most time-consuming calculations are the quark-gluon vertex integrals; not because they are hard to do by themselves, but rather because they have to be performed millions of times, and each integral contains products of three spherical Bessel functions. Gaussian quadrature is applied here, since it is the most efficient numerical integration method [53]. The integrals are all of the form

$$\int_0^1 r^2 j_l(x_n r)\, j_{l'}(x_{n'} r)\, j_J(y_m r)\, dr. \tag{C.3}$$

Since the integrand is highly oscillatory, 50 integration points are used. The weights and abscissae are calculated at the beginning of each program and are then used for all the integrals.

C.4 Angular Momenta

The 3j-symbols appearing in the quark-gluon vertex integrals are calculated using the series expansion derived by Racah [54] as given in the book by Edmonds. [51. Equation (3.6.11)]. They describe the coupling at each vertex.

In the second order terms, one can combine two of the 3j-symbols by using the

identity

$$\sum_{\mu_q} \begin{pmatrix} j_f & J_1 & j_q \\ -\mu_f & M_1 & -\mu_q \end{pmatrix} \begin{pmatrix} j_q & J_2 & j_i \\ \mu_q & M_2 & \mu_i \end{pmatrix} = \sum_{\Lambda\lambda} (2\Lambda+1)(-1)^{\phi} \begin{Bmatrix} j_f & J_1 & j_q \\ J_2 & j_i & \Lambda \end{Bmatrix} \begin{pmatrix} j_f & \Lambda & j_i \\ -\mu_f & \lambda & \mu_i \end{pmatrix} \begin{pmatrix} J_1 & J_2 & \Lambda \\ M_1 & M_2 & -\lambda \end{pmatrix}, \tag{C.4}$$

where the phase ϕ is

$$\phi = j_f + j_i + J_1 + J_2 - j_q + \Lambda + \mu_f - M_2. \tag{C.5}$$

One also makes use of the completeness relation for 3j-symbols

$$\sum_{M_1 M_2} \begin{pmatrix} J_1 & J_2 & \Lambda \\ M_1 & M_2 & \lambda \end{pmatrix} \begin{pmatrix} J_1 & J_2 & \Lambda' \\ M_1 & M_2 & \lambda' \end{pmatrix} = \frac{\delta_{\Lambda\Lambda'}\delta_{\lambda\lambda'}}{2\Lambda+1}. \tag{C.6}$$

6j-symbols appear in the second order terms when one combines the two interactions into one apparent interaction. One encounters two types of 6j-symbols, which differ in the total angular momentum exchanged, Λ. The first, with total angular momentum 0, is readily evaluated.

$$\begin{Bmatrix} \frac{1}{2} & J_1 & j_q \\ J_2 & \frac{1}{2} & 0 \end{Bmatrix} = \frac{(-1)^{\frac{1}{2}+j_q+J_2}\delta_{J_1 J_2}}{\sqrt{2(2J_1+1)}}. \tag{C.7}$$

The 6j-symbols for $\Lambda = 1$ need to be evaluated numerically, however. The routines used are based on the series expansions given again in [51, Table 5].

Appendix D

Energy Denominators

Due to their length, the expressions for the energy denominators for the two-gluon exchange have been taken out of the main part of the thesis.

D.1 The "Straight" Two-Gluon Exchange Diagram

$$
\begin{aligned}
E_{\mathrm{I}} \;=\; & \Big[(\varepsilon_{q'}-\varepsilon_{i'}+\Omega^{\Sigma'}_{m'})(\varepsilon_{f'}-\varepsilon_{i'}+\Omega^{\Sigma}_{m}+\Omega^{\Sigma'}_{m'})(\varepsilon_{q}-\varepsilon_{f}+\Omega^{\Sigma}_{m})\Big]^{-1} \\
& + \Big[(\varepsilon_{q'}-\varepsilon_{i'}+\Omega^{\Sigma'}_{m'})(\varepsilon_{q}+\varepsilon_{q'}-\varepsilon_{i}-\varepsilon_{i'})(\varepsilon_{q}-\varepsilon_{f}+\Omega^{\Sigma}_{m})\Big]^{-1} \\
& + \Big[(\varepsilon_{q}-\varepsilon_{i}+\Omega^{\Sigma'}_{m'})(\varepsilon_{q}+\varepsilon_{q'}-\varepsilon_{i}-\varepsilon_{i'})(\varepsilon_{q}-\varepsilon_{f}+\Omega^{\Sigma}_{m})\Big]^{-1} \\
& + \Big[(\varepsilon_{q'}-\varepsilon_{i'}+\Omega^{\Sigma'}_{m'})(\varepsilon_{q}+\varepsilon_{q'}-\varepsilon_{i}-\varepsilon_{i'})(\varepsilon_{q'}-\varepsilon_{f'}+\Omega^{\Sigma}_{m})\Big]^{-1} \\
& + \Big[(\varepsilon_{q}-\varepsilon_{i}+\Omega^{\Sigma'}_{m'})(\varepsilon_{q}+\varepsilon_{q'}-\varepsilon_{i}-\varepsilon_{i'}+)(\varepsilon_{q'}-\varepsilon_{f'}+\Omega^{\Sigma}_{m})\Big]^{-1} \\
& + \Big[(\varepsilon_{q}-\varepsilon_{i}+\Omega^{\Sigma'}_{m'})(\varepsilon_{f}-\varepsilon_{i}+\Omega^{\Sigma}_{m}+\Omega^{\Sigma'}_{m'})(\varepsilon_{q'}-\varepsilon_{f'}+\Omega^{\Sigma}_{m})\Big]^{-1}
\end{aligned}
\tag{D.1}
$$

$$
\begin{aligned}
E_{\mathrm{II}} \;=\; & \Big[(\varepsilon_{q'}+\varepsilon_{f'}+\Omega^{\Sigma}_{m})(\varepsilon_{f'}-\varepsilon_{i'}+\Omega^{\Sigma}_{m}+\Omega^{\Sigma'}_{m'})(\varepsilon_{q}-\varepsilon_{f}+\Omega^{\Sigma}_{m})\Big]^{-1} \\
& + \Big[(\varepsilon_{q'}+\varepsilon_{f'}+\Omega^{\Sigma}_{m})(\varepsilon_{f'}-\varepsilon_{i}+\varepsilon_{q}+\varepsilon_{q'}+\Omega^{\Sigma}_{m}+\Omega^{\Sigma'}_{m'})(\varepsilon_{q}-\varepsilon_{f}+\Omega^{\Sigma}_{m})\Big]^{-1} \\
& + \Big[(\varepsilon_{q}-\varepsilon_{i}+\Omega^{\Sigma'}_{m'})(\varepsilon_{f'}-\varepsilon_{i}+\varepsilon_{q}+\varepsilon_{q'}+\Omega^{\Sigma}_{m}+\Omega^{\Sigma'}_{m'})(\varepsilon_{q}-\varepsilon_{f}+\Omega^{\Sigma}_{m})\Big]^{-1} \\
& + \Big[(\varepsilon_{q'}+\varepsilon_{f'}+\Omega^{\Sigma}_{m})(\varepsilon_{f'}-\varepsilon_{i}+\varepsilon_{q}+\varepsilon_{q'}+\Omega^{\Sigma}_{m}+\Omega^{\Sigma'}_{m'})(\varepsilon_{q'}+\varepsilon_{i'}+\Omega^{\Sigma'}_{m'})\Big]^{-1} \\
& + \Big[(\varepsilon_{q}-\varepsilon_{i}+\Omega^{\Sigma'}_{m'})(\varepsilon_{f'}-\varepsilon_{i}+\varepsilon_{q}+\varepsilon_{q'}+\Omega^{\Sigma}_{m}+\Omega^{\Sigma'}_{m'})(\varepsilon_{q'}+\varepsilon_{i'}+\Omega^{\Sigma'}_{m'})\Big]^{-1} \\
& + \Big[(\varepsilon_{q}-\varepsilon_{i}+\Omega^{\Sigma'}_{m'})(\varepsilon_{f}-\varepsilon_{i}+\Omega^{\Sigma}_{m}+\Omega^{\Sigma'}_{m'})(\varepsilon_{q'}+\varepsilon_{i'}+\Omega^{\Sigma'}_{m'})\Big]^{-1}
\end{aligned}
\tag{D.2}
$$

$$
\begin{aligned}
E_{\rm III} \;=\;& \Big[(\varepsilon_{q'}-\varepsilon_{i'}+\Omega^{\Sigma'}_{m'})(\varepsilon_{f'}-\varepsilon_{i'}+\Omega^{\Sigma}_{m}+\Omega^{\Sigma'}_{m'})(\varepsilon_{q}+\varepsilon_{i}+\Omega^{\Sigma'}_{m'})\Big]^{-1} \\
&+\Big[(\varepsilon_{q'}-\varepsilon_{i'}+\Omega^{\Sigma'}_{m'})(\varepsilon_{f}-\varepsilon_{i'}+\varepsilon_{q}+\varepsilon_{q'}+\Omega^{\Sigma}_{m}+\Omega^{\Sigma'}_{m'})(\varepsilon_{q}+\varepsilon_{i}+\Omega^{\Sigma'}_{m'})\Big]^{-1} \\
&+\Big[(\varepsilon_{q'}-\varepsilon_{i'}+\Omega^{\Sigma'}_{m'})(\varepsilon_{f}-\varepsilon_{i'}+\varepsilon_{q}+\varepsilon_{q'}+\Omega^{\Sigma}_{m}+\Omega^{\Sigma'}_{m'})(\varepsilon_{q'}-\varepsilon_{f'}+\Omega^{\Sigma}_{m})\Big]^{-1} \\
&+\Big[(\varepsilon_{q}+\varepsilon_{f}+\Omega^{\Sigma}_{m})(\varepsilon_{f}-\varepsilon_{i'}+\varepsilon_{q}+\varepsilon_{q'}+\Omega^{\Sigma}_{m}+\Omega^{\Sigma'}_{m'})(\varepsilon_{q}+\varepsilon_{i}+\Omega^{\Sigma'}_{m'})\Big]^{-1} \\
&+\Big[(\varepsilon_{q}+\varepsilon_{f}+\Omega^{\Sigma}_{m})(\varepsilon_{f}-\varepsilon_{i'}+\varepsilon_{q}+\varepsilon_{q'}+\Omega^{\Sigma}_{m}+\Omega^{\Sigma'}_{m'})(\varepsilon_{q'}-\varepsilon_{f'}+\Omega^{\Sigma}_{m})\Big]^{-1} \\
&+\Big[(\varepsilon_{q}+\varepsilon_{f}+\Omega^{\Sigma}_{m})(\varepsilon_{f}-\varepsilon_{i}+\Omega^{\Sigma}_{m}+\Omega^{\Sigma'}_{m'})(\varepsilon_{q'}-\varepsilon_{f'}+\Omega^{\Sigma}_{m})\Big]^{-1}
\end{aligned}
\tag{D.3}
$$

$$
\begin{aligned}
E_{\rm IV} \;=\;& \Big[(\varepsilon_{q'}+\varepsilon_{f'}+\Omega^{\Sigma}_{m})(\varepsilon_{f'}-\varepsilon_{i'}+\Omega^{\Sigma}_{m}+\Omega^{\Sigma'}_{m'})(\varepsilon_{q}+\varepsilon_{i}+\Omega^{\Sigma'}_{m'})\Big]^{-1} \\
&+\Big[(\varepsilon_{q'}+\varepsilon_{f'}+\Omega^{\Sigma}_{m})(\varepsilon_{f}+\varepsilon_{f'}+\varepsilon_{q}+\varepsilon_{q'})(\varepsilon_{q}+\varepsilon_{i}+\Omega^{\Sigma'}_{m'})\Big]^{-1} \\
&+\Big[(\varepsilon_{q}+\varepsilon_{f}+\Omega^{\Sigma}_{m})(\varepsilon_{f}+\varepsilon_{f'}+\varepsilon_{q}+\varepsilon_{q'})(\varepsilon_{q}+\varepsilon_{i}+\Omega^{\Sigma'}_{m'})\Big]^{-1} \\
&+\Big[(\varepsilon_{q'}+\varepsilon_{f'}+\Omega^{\Sigma}_{m})(\varepsilon_{f}+\varepsilon_{f'}+\varepsilon_{q}+\varepsilon_{q'})(\varepsilon_{q'}+\varepsilon_{i'}+\Omega^{\Sigma'}_{m'})\Big]^{-1} \\
&+\Big[(\varepsilon_{q}+\varepsilon_{f}+\Omega^{\Sigma}_{m})(\varepsilon_{f}+\varepsilon_{f'}+\varepsilon_{q}+\varepsilon_{q'})(\varepsilon_{q'}+\varepsilon_{i'}+\Omega^{\Sigma'}_{m'})\Big]^{-1} \\
&+\Big[(\varepsilon_{q}+\varepsilon_{f}+\Omega^{\Sigma}_{m})(\varepsilon_{f}-\varepsilon_{i}+\Omega^{\Sigma}_{m}+\Omega^{\Sigma'}_{m'})(\varepsilon_{q'}+\varepsilon_{i'}+\Omega^{\Sigma'}_{m'})\Big]^{-1}
\end{aligned}
\tag{D.4}
$$

D.2 The "Crossed" Two-Gluon Exchange Diagram

$$
\begin{aligned}
E_{\rm I} \;=\;& \Big[(\varepsilon_{q'}-\varepsilon_{i'}+\Omega^{\Sigma}_{m})(\varepsilon_{f'}-\varepsilon_{i'}+\Omega^{\Sigma}_{m}+\Omega^{\Sigma'}_{m'})(\varepsilon_{q}-\varepsilon_{f}+\Omega^{\Sigma}_{m})\Big]^{-1} \\
&+\Big[(\varepsilon_{q'}-\varepsilon_{i'}+\Omega^{\Sigma}_{m})(\varepsilon_{q}+\varepsilon_{q'}-\varepsilon_{i}-\varepsilon_{i'}+\Omega^{\Sigma}_{m}+\Omega^{\Sigma'}_{m'})(\varepsilon_{q}-\varepsilon_{f}+\Omega^{\Sigma}_{m})\Big]^{-1} \\
&+\Big[(\varepsilon_{q}-\varepsilon_{i}+\Omega^{\Sigma'}_{m'})(\varepsilon_{q}+\varepsilon_{q'}-\varepsilon_{i}-\varepsilon_{i'}+\Omega^{\Sigma}_{m}+\Omega^{\Sigma'}_{m'})(\varepsilon_{q}-\varepsilon_{f}+\Omega^{\Sigma}_{m})\Big]^{-1} \\
&+\Big[(\varepsilon_{q'}-\varepsilon_{i'}+\Omega^{\Sigma}_{m})(\varepsilon_{q}+\varepsilon_{q'}-\varepsilon_{i}-\varepsilon_{i'}+\Omega^{\Sigma}_{m}+\Omega^{\Sigma'}_{m'})(\varepsilon_{q'}-\varepsilon_{f'}+\Omega^{\Sigma'}_{m'})\Big]^{-1} \\
&+\Big[(\varepsilon_{q}-\varepsilon_{i}+\Omega^{\Sigma'}_{m'})(\varepsilon_{q}+\varepsilon_{q'}-\varepsilon_{i}-\varepsilon_{i'}+\Omega^{\Sigma}_{m}+\Omega^{\Sigma'}_{m'})(\varepsilon_{q'}-\varepsilon_{f'}+\Omega^{\Sigma'}_{m'})\Big]^{-1} \\
&+\Big[(\varepsilon_{q}-\varepsilon_{i}+\Omega^{\Sigma'}_{m'})(\varepsilon_{f}-\varepsilon_{i}+\Omega^{\Sigma}_{m}+\Omega^{\Sigma'}_{m'})(\varepsilon_{q'}-\varepsilon_{f'}+\Omega^{\Sigma'}_{m'})\Big]^{-1}
\end{aligned}
\tag{D.5}
$$

$$
\begin{aligned}
E_{\rm II} \;=\;& \Big[(\varepsilon_{q'}+\varepsilon_{f'}+\Omega^{\Sigma'}_{m'})(\varepsilon_{f'}-\varepsilon_{i'}+\Omega^{\Sigma}_{m}+\Omega^{\Sigma'}_{m'})(\varepsilon_{q}-\varepsilon_{f}+\Omega^{\Sigma}_{m})\Big]^{-1} \\
&+\Big[(\varepsilon_{q'}+\varepsilon_{f'}+\Omega^{\Sigma'}_{m'})(\varepsilon_{q}+\varepsilon_{q'}+\varepsilon_{f'}-\varepsilon_{i})(\varepsilon_{q}-\varepsilon_{f}+\Omega^{\Sigma}_{m})\Big]^{-1} \\
&+\Big[(\varepsilon_{q}-\varepsilon_{i}+\Omega^{\Sigma'}_{m'})(\varepsilon_{q}+\varepsilon_{q'}+\varepsilon_{f'}-\varepsilon_{i})(\varepsilon_{q}-\varepsilon_{f}+\Omega^{\Sigma}_{m})\Big]^{-1} \\
&+\Big[(\varepsilon_{q'}+\varepsilon_{f'}+\Omega^{\Sigma'}_{m'})(\varepsilon_{q}+\varepsilon_{q'}+\varepsilon_{f'}-\varepsilon_{i})(\varepsilon_{q'}+\varepsilon_{i'}+\Omega^{\Sigma}_{m})\Big]^{-1} \\
&+\Big[(\varepsilon_{q}-\varepsilon_{i}+\Omega^{\Sigma'}_{m'})(\varepsilon_{q}+\varepsilon_{q'}+\varepsilon_{f'}-\varepsilon_{i})(\varepsilon_{q'}+\varepsilon_{i'}+\Omega^{\Sigma}_{m})\Big]^{-1} \\
&+\Big[(\varepsilon_{q}-\varepsilon_{i}+\Omega^{\Sigma'}_{m'})(\Omega^{\Sigma}_{m}+\Omega^{\Sigma'}_{m'}+\varepsilon_{f}-\varepsilon_{i})(\varepsilon_{q'}+\varepsilon_{i'}+\Omega^{\Sigma}_{m})\Big]^{-1}
\end{aligned}
\tag{D.6}
$$

$$
\begin{aligned}
E_{\rm III} \;=\;& \Big[(\varepsilon_{q'}-\varepsilon_{i'}+\Omega^{\Sigma}_{m})(\varepsilon_{f'}-\varepsilon_{i'}+\Omega^{\Sigma}_{m}+\Omega^{\Sigma'}_{m'})(\varepsilon_{q}+\varepsilon_{i}+\Omega^{\Sigma'}_{m'})\Big]^{-1} \\
&+\Big[(\varepsilon_{q'}-\varepsilon_{i'}+\Omega^{\Sigma}_{m})(\varepsilon_{q}+\varepsilon_{q'}+\varepsilon_{f}-\varepsilon_{i'})(\varepsilon_{q}+\varepsilon_{i}+\Omega^{\Sigma'}_{m'})\Big]^{-1} \\
&+\Big[(\varepsilon_{q'}-\varepsilon_{i'}+\Omega^{\Sigma}_{m})(\varepsilon_{q}+\varepsilon_{q'}+\varepsilon_{f}-\varepsilon_{i'})(\varepsilon_{q'}-\varepsilon_{f'}+\Omega^{\Sigma'}_{m'})\Big]^{-1} \\
&+\Big[(\varepsilon_{q}+\varepsilon_{f}+\Omega^{\Sigma}_{m})(\varepsilon_{q}+\varepsilon_{q'}+\varepsilon_{f}-\varepsilon_{i'})(\varepsilon_{q}+\varepsilon_{i}+\Omega^{\Sigma'}_{m'})\Big]^{-1} \\
&+\Big[(\varepsilon_{q}+\varepsilon_{f}+\Omega^{\Sigma}_{m})(\varepsilon_{q}+\varepsilon_{q'}+\varepsilon_{f}-\varepsilon_{i'})(\varepsilon_{q'}-\varepsilon_{f'}+\Omega^{\Sigma'}_{m'})\Big]^{-1} \\
&+\Big[(\varepsilon_{q}+\varepsilon_{f}+\Omega^{\Sigma}_{m})(\varepsilon_{f}-\varepsilon_{i}+\Omega^{\Sigma}_{m}+\Omega^{\Sigma'}_{m'})(\varepsilon_{q'}-\varepsilon_{f'}+\Omega^{\Sigma'}_{m'})\Big]^{-1}
\end{aligned}
\tag{D.7}
$$

$$
\begin{aligned}
E_{\rm IV} \;=\;& \Big[(\varepsilon_{q'}+\varepsilon_{f'}+\Omega^{\Sigma'}_{m'})(\varepsilon_{f'}-\varepsilon_{i'}+\Omega^{\Sigma}_{m}+\Omega^{\Sigma'}_{m'})(\varepsilon_{q}+\varepsilon_{i}+\Omega^{\Sigma'}_{m'})\Big]^{-1} \\
&+\Big[(\varepsilon_{q'}+\varepsilon_{f'}+\Omega^{\Sigma'}_{m'})(\varepsilon_{q}+\varepsilon_{q'}+\varepsilon_{f}+\varepsilon_{f'}+\Omega^{\Sigma}_{m}+\Omega^{\Sigma'}_{m'})(\varepsilon_{q}+\varepsilon_{i}+\Omega^{\Sigma'}_{m'})\Big]^{-1} \\
&+\Big[(\varepsilon_{q}+\varepsilon_{f}+\Omega^{\Sigma}_{m})(\varepsilon_{q}+\varepsilon_{q'}+\varepsilon_{f}+\varepsilon_{f'}+\Omega^{\Sigma}_{m}+\Omega^{\Sigma'}_{m'})(\varepsilon_{q}+\varepsilon_{i}+\Omega^{\Sigma'}_{m'})\Big]^{-1} \\
&+\Big[(\varepsilon_{q'}+\varepsilon_{f'}+\Omega^{\Sigma'}_{m'})(\varepsilon_{q}+\varepsilon_{q'}+\varepsilon_{f}+\varepsilon_{f'}+\Omega^{\Sigma}_{m}+\Omega^{\Sigma'}_{m'})(\varepsilon_{q'}+\varepsilon_{i'}+\Omega^{\Sigma}_{m})\Big]^{-1} \\
&+\Big[(\varepsilon_{q}+\varepsilon_{f}+\Omega^{\Sigma}_{m})(\varepsilon_{q}+\varepsilon_{q'}+\varepsilon_{f}+\varepsilon_{f'}+\Omega^{\Sigma}_{m}+\Omega^{\Sigma'}_{m'})(\varepsilon_{q'}+\varepsilon_{i'}+\Omega^{\Sigma}_{m})\Big]^{-1} \\
&+\Big[(\varepsilon_{q}+\varepsilon_{f}+\Omega^{\Sigma}_{m})(\varepsilon_{f}-\varepsilon_{i}+\Omega^{\Sigma}_{m}+\Omega^{\Sigma'}_{m'})(\varepsilon_{q'}+\varepsilon_{i'}+\Omega^{\Sigma}_{m})\Big]^{-1}
\end{aligned}
\tag{D.8}
$$

Bibliography

[1] Fritzsch, H., Gell-Mann, M., and Leutwyler, H. *Phys. Lett. B* **47**, 365 (1973).

[2] Friedman, J. T. and Kendall, H. W. *Ann. Rev. Nucl. Science* **22**, 203 (1972).

[3] Taylor, J. C. *Nucl. Phys. B* **33**, 436 (1971).

[4] Bjorken, J. D. and Paschos, E. A. *Phys. Rev.* **185**, 1957 (1969).

[5] Gross, D. J. and Wilczek, F. *Phys. Rev. D* **8**, 3633 (1973).

[6] Gross, D. J. and Wilczek, F. *Phys. Rev. Lett.* **30**, 1343 (1973).

[7] Politzer, H. D. *Phys. Rev. Lett.* **30**, 1346 (1973).

[8] 't Hooft, G. *Nucl. Phys. B* **33**, 173 (1971).

[9] 't Hooft, G. *Nucl. Phys. B* **35**, 167 (1971).

[10] Friedberg, R. and Lee, T. D. *Phys. Rev. D* **15**, 1694 (1977).

[11] Friedberg, R. and Lee, T. D. *Phys. Rev. D* **16**, 1096 (1977).

[12] Friedberg, R. and Lee, T. D. *Phys. Rev. D* **18**, 2623 (1978).

[13] Vento, V., Rho, M., Nyman, E. M., Jun, J. H., and Brown, G. E. *Nucl. Phys. A* **345**, 413 (1980).

[14] Miller, G. A., Thomas, A. W., and Théberge, S. *Phys. Lett. B* **91**, 192 (1980).

[15] Théberge, S., Thomas, A. W., and Miller, G. A. *Phys. Rev. D* **22**, 2838 (1980).

[16] Thomas, A. W., Théberge, S., and Miller, G. A. *Phys. Rev. D* **24**, 216 (1981).

[17] Chodos, A., Jaffe, R. L., Johnson, K., Thorn, C. B., and Weisskopf, V. F. *Phys. Rev. D* **9**, 3471 (1974).

[18] Chodos, A., Jaffe, R. L., Johnson, K., and Thorn, C. B. *Phys. Rev. D* **10**, 2599 (1974).

[19] DeGrand, T., Jaffe, R. L., Johnson, K., and Kiskis, J. *Phys. Rev. D* **12**, 2060 (1975).

[20] Johnson, K. *Acta Physica Polonica B* **6**, 865 (1975).

[21] Buser, R. F., Viollier, R. D., and Zimak, P. *Int. J. Theo. Phys.* **27**, 925 (1988).

[22] Stoddart, A. J. *Renormalization of Cavity Field Theories.* PhD thesis, University of Cape Town (1989).

[23] Stoddart, A. J. and Viollier, R. D. *Phys. Lett. B* **236**, 387 (1990).

[24] Stoddart, A. J. and Viollier, R. D. *Nucl. Phys. A* **532**, 657 (1991).

[25] Stoddart, A. J. and Viollier, R. D. *Nucl. Phys. A* **541**, 623 (1992).

[26] Cuthbert, J. A. *Massive Quark Self-Energy in Cavity QCD.* Master's thesis, University of Cape Town (1991).

[27] Cuthbert, J. A. and Viollier, R. D. *Z. Phys. C* **58**, 295 (1993).

[28] Schreiber, G. U. *The Gluon Self-Energy in Cavity QCD.* PhD thesis, University of Cape Town (1991).

[29] Schreiber, G. U. and Viollier, R. D. *Ann. of Phys.* **215**, 277 (1992).

[30] Schreiber, G. U. and Viollier, R. D. *Phys. Lett. B* **279**, 131 (1992).

[31] O'Connor, M. S. *The Anomalous Magnetic Moment of the Nucleon in Cavity QCD.* PhD thesis, University of Cape Town (1991).

[32] O'Connor, M. S. and Viollier, R. D. *Ann. of Phys.* **248**, 286 (1996).

[33] Lindebaum, R. J. *The Anomalous Magnetic Moment of Baryons in Cavity QCD.* Master's thesis, University of Cape Town (1992).

[34] Page, P. R. *The Ratio g_A/g_V in Cavity QCD.* Master's thesis, University of Cape Town (1991).

[35] Page, P. R., Lindebaum, R. J., and Viollier, R. D. *Nucl. Phys. A* **560**, 1003 (1993).

[36] Stoddart, A. J. *Perturbative Quantum Chromodynamics in a Cavity.* Master's thesis, University of Cape Town (1987).

[37] Stoddart, A. J. and Viollier, R. D. *Phys. Lett. B* **208**, 65 (1988).

[38] Greiner, W. and Schäfer, A. *Quantum Chromodynamics.* Springer, Berlin, 2nd edition (1995).

[39] Fadeev, L. D. and Popov, V. N. *Phys. Lett. B* **25**, 29 (1967).

[40] Becchi, C., Rouet, A., and Stora, R. *Phys. Lett. B* **52**, 344 (1974).

[41] Feynman, R. P. *Rev. Mod. Phys.* **20**, 367 (1948).

[42] Gupta, S. N. *Proc. Phys. Soc. A* **367**, 681 (1950).

[43] Bleuler, K. *H. P. A.* **23**, 367 (1950).

[44] Kugo, T. and Ojima, I. *Prog. Theo. Phys.* **60**, 1869 (1978).

[45] Viollier, R. D., Chin, S. A., and Kerman, A. K. *Nucl. Phys. A* **407**, 269 (1983).

[46] Gell-Mann, M. and Low, F. *Phys. Rev.* **84**, 350 (1951).

[47] Fetter, A. L. and Walecka, J. D. *Quantum Theory of Many-Particle Systems.* McGraw-Hill, New York (1971).

[48] Sucher, J. *Phys. Rev.* **107**, 1448 (1957).

[49] Plunien, G., Müller, B., and Greiner, W. *Phys. Rep.* **134**, 87 (1986).

[50] D. R. Thomson *et al.* (E852 Collab.). *Phys. Rev. Lett.* **79**, 1630 (1997).

[51] Edmonds, A. R. *Angular Momentum in Quantum Mechanics.* Princeton University Press, New Jersey (1957).

[52] Gillman, E. and Fiebig, H. R. *Computers in Physics* **2**, 62 (1988).

[53] Press, W. H. *et al.*. *Numerical Recipes.* Cambridge University Press, Cambridge (1988).

[54] Racah, G. *Phys. Rev.* **62**, 438 (1942).